



NIWA
Taihoro Nukurangi

Evaluating surrogate technologies for river suspended sediment load monitoring

Prepared for Envirolink

August 2023

Prepared by:

Arman Haddadchi, Andrew Willsman, John Montgomery

For any information regarding this report please contact:




Arman Haddadchi
Sediment Transport Scientist
Group
+64-3-343 7896
arman.haddadchi@niwa.co.nz

National Institute of Water & Atmospheric Research Ltd
PO Box 8602
Riccarton
Christchurch 8440

Phone +64 3 348 8987

NIWA CLIENT REPORT No: 2023239CH
Report date: August 2023
NIWA Project: ELF20502

Revision	Description	Date
Version 1.0	Final report to client	28 August 2023

Quality Assurance Statement		
	Reviewed by:	Neale Hudson
	Formatting checked by:	Rachel Wright
	Approved for release by:	Charles Pearson

© All rights reserved. This publication may not be reproduced or copied in any form without the permission of the copyright owner(s). Such permission is only to be given in accordance with the terms of the client's contract with NIWA. This copyright extends to all forms of copying and any storage of material in any kind of information retrieval system.

Whilst NIWA has used all reasonable endeavours to ensure that the information contained in this document is accurate, NIWA does not give any express or implied warranty as to the completeness of the information contained herein, or that it will be suitable for any purpose(s) other than those specifically contemplated during the Project or agreed by NIWA and the Client.

Contents

- Executive summary 6**

- 1 Introduction 9**
 - 1.1 Background 9
 - 1.2 Project brief 10
 - 1.3 Scope of the project..... 10

- 2 Data 12**
 - 2.1 Surrogate sensors 12
 - 2.2 Sediment sampling 14

- 3 Analysis method 19**
 - 3.1 Approach..... 19
 - 3.2 At-a-point SSC measurements against cross-section averaged SSC..... 19
 - 3.3 Turbidity data measurements 19
 - 3.4 At-a-point acoustic measurements 20
 - 3.5 Side-looking acoustic measurements 20
 - 3.6 Evaluating performance of the surrogate sensors in estimating sediment load.... 22

- 4 Results 23**
 - 4.1 The results of calibrating at-a-point SSC to cross-section averaged SSC..... 23
 - 4.2 The results of calibrating turbidity measurements 26
 - 4.3 The results of calibrating at-a-point ABS measurements 31
 - 4.4 Calibration of side-looking acoustic data using SAID toolbox 34
 - 4.5 Assessing performance of surrogate methods in sediment load estimation 39

- 5 Summary and recommendations 48**
 - 5.1 The need to calibrate auto-sampled SSC to cross-section averaged SSC..... 48
 - 5.2 Sediment concentration measurements using turbidity sensors..... 48
 - 5.3 Sediment concentration measurements using at-a-point acoustic backscatter sensors 50
 - 5.4 Assessing performance of surrogate methods in sediment load estimation 51
 - 5.5 Field experience with use of surrogate technologies 53

- 6 Acknowledgements 58**

7	Glossary of abbreviations and terms	59
8	References.....	60
Appendix A	Figure A-3Side-looking acoustic measurements.....	62

Tables

Table 2-1:	Characteristics of catchments upstream of the monitoring sites and a list of surrogate instruments used at each site.	13
Table 2-2:	Summary of collected suspended sediment samples and flow measurements at monitoring sites.	17
Table 4-1:	Regression characteristics and uncertainties in relationship between auto-sampled SSC and turbidity for all monitoring sites.	31
Table 4-2:	Regression characteristics and uncertainties in relationship between auto-sampled SSC and at-a-point acoustic (LISST-ABS) for Mataura River and Manawatu River.	33
Table 4-3:	Configuration and processing parameters to calculate acoustic surrogates.	34
Table 4-4:	Linear regression model statistics for the SSC measurements using side-looking ADCP sensors at all four monitored rivers.	37
Table 4-5:	Comparing the performance of surrogate techniques in estimating suspended sediment load.	46
Table 5-1:	Comparing side-looking and at-a-point optical and acoustic sensors.	55

Figures

Figure 2-1:	Side-looking acoustic backscatter profilers deployed at the monitoring sites.	14
Figure 2-2:	Example of depth-integrated physical sampling in Oreti River .	16
Figure 2-3:	Continuous flow records and sediment samples used to calibrate the surrogate sensors at all monitoring rivers.	17
Figure 4-1:	Relationship between auto-sampled and gauged cross-section .	23
Figure 4-2:	Relationship between auto-sampled and gauged cross-section average SSC for three size fraction classes.	24
Figure 4-3:	Relationship between auto-sampled and gauged cross-section average SSC for three size fraction classes.	25
Figure 4-4:	Relationship between auto-sampled and gauged cross-section average SSC for three size fraction classes:.	26
Figure 4-5:	Relationship between auto-sampled SSC and field turbidity for three size fraction classes:.	27
Figure 4-6:	Relationship between auto-sampled SSC and field turbidity for three size fraction classes:.	28
Figure 4-7:	Relationship between auto-sampled SSC and field turbidity for three size fraction classes:.	29
Figure 4-8:	Relationship between auto-sampled SSC and field turbidity for three size fraction classes:.	30
Figure 4-9:	Relationship between auto-sampled SSC and at-a-point acoustic measurements for three size fraction classes: .	32

Figure 4-10:	Relationship between auto-sampled SSC and at-a-point acoustic measurements for three size fraction classes: .	33
Figure 4-11:	Backscatter profile of the Acoustic Doppler Velocity Meter .	36
Figure 4-12:	Linear regression plot of the log ₁₀ SSC against mean sediment corrected backscatter of all four monitored rivers.	37
Figure 4-13:	Flood events together with collected sediment samples used to evaluate performance of surrogate methods in estimating sediment load at the Oreti River.	40
Figure 4-14:	Turbidity-derived SSC, ABS side-looking-derived SSC and flow data for selected flood .	41
Figure 4-15:	Flood events and collected sediment samples used to evaluate performance of surrogate methods in estimating sediment load at the Mataura River.	42
Figure 4-16:	Turbidity-derived SSC.	43
Figure 4-17:	Flood event and collected sediment samples used to evaluate performance of surrogate methods in estimating sediment load at the Manawatu River.	44
Figure 4-18:	Turbidity-derived SSC, at-a-point ABS-derived SSC, ABS side-looking-derived SSC and flow data for selected flood events in the Manawatu River.	44
Figure 4-19:	Flood event and collected sediment samples used to evaluate performance of surrogate methods in estimating sediment load at the Grey River..	45
Figure 4-20:	Turbidity-derived SSC, ABS side-looking-derived SSC and flow data for selected flood events .	46
Figure 5-1:	Turbidity measurements from four different sensors during November 2019 event at the Mataura River.	49
Figure 5-2:	Saturation of turbidity sensor during high flows in Rangitata River at Gorge site.	50
Figure 5-3:	Data acquired during a flood in Mataura River showing patterns of sediment movement during the event.	51
Figure 5-4:	Average SSC (left plots) and its cross-sectional variation (right plots) in two example floods at the Oreti River.	52
Figure 5-5:	Variation of SSC at four bins during the two example floods at the Oreti River.	53
Figure 5-6:	A sliding rail mount at Mataura River and cleaning the sensor by Andrew Willsman (NIWA-Dunedin).	55

Executive summary

Reducing the impact of suspended sediment on aquatic habitats requires monitoring of suspended sediment loads – both to assist in directing catchment erosion mitigation work, and in measuring the efficacy of the mitigation and determining whether or not catchment load limits are being met. Identifying a ‘field-effective’ surrogate for high frequency monitoring of suspended sediment concentration (SSC) in different riverine environments is a prerequisite for better monitoring of sediment concentrations and for estimating the sediment load. The data derived from enhanced monitoring will inform policy implementation in matters relating to sediment, and assist stakeholders (including Māori) to predict and better assess the effects of sediment transport and deposition, so that the condition of freshwater and estuarine environments may be improved.

Continuous suspended sediment monitoring in New Zealand rivers over the last several decades has typically utilised optical sensors that measure turbidity as a surrogate for SSC. Acoustic backscatter provides an alternative technology offering significant advantages over the more traditional optical method.

NIWA was commissioned by MBIE through the Envirolink scheme to provide guidance on the selection of appropriate surrogate monitoring technologies for robust measurement of the suspended sediment load to support freshwater and coastal management. This report briefly describes several technologies that provide surrogate estimates of suspended sediment concentration. Thereafter, the performance of surrogate technologies for measurement of the suspended sediment concentration and load is described using several types of instrumentation deployed at four representative New Zealand rivers. The surrogate technologies tested in this study include:

- a range of optical turbidity instruments, as well as
- point and profiling acoustic back-scatter instruments.

In addition to evaluating sensor performance, experience and knowledge from instrument set-up and generation of fit for purpose information is provided. This information may be used to guide practitioners working in rivers having different sediment characteristics (e.g., sand vs mud-dominated, varying suspended sediment concentration ranges) where suspended sediment concentration and load information is required.

The primary users of the information in this report are likely to be Regional Councils and Unitary authorities who are commencing, expanding, or rationalising suspended sediment monitoring programs, and who require time-series records of SSC to meet their monitoring and policy objectives. Access to the information that will be provided by this Tool is a priority for them because:

- there are obligations under the National Policy Statement for Freshwater Management to manage sediment loads and sediment-related environmental attributes (e.g., visual clarity, deposited fine sediment), for which considerably more sophisticated data will be required,
- relatively limited and “patchy” information is available regarding:
 - surrogate technology options, notably in regard to what technology is best suited for particular rivers (e.g., mud or sand-dominated suspended loads),

- what use can be made of existing multi-purpose instrumentation (e.g., side-looking ADCPs, Acoustic Doppler Current Profilers), and
- how acoustic surrogate data are best analysed (e.g., the processing of ADCP backscatter records is not trivial and will require some resource investment and training to begin utilisation of these data for high frequency sediment monitoring).

The current state of knowledge regarding use of surrogate technologies for estimating suspended sediment concentrations and loads, along with some bad experiences (poor-quality data derived from previous turbidity sensor deployments), has discouraged investment in updated suspended sediment monitoring programs, including implementation of new technology.

The key findings obtained from review and comparison of data derived from different surrogate sensors are:

- A comparison between the relationships of at-a-point SSC collected by autosamplers, and cross-section averaged depth-integrated SSC obtained through physical sediment samplers (such as depth-integrated or point-integrated samplers) indicate that the cross-section averaged SSC does not align with the at-a-point SSC estimates; reasons include:
 - uneven mixing of the suspended sediment load throughout the cross section,
 - variations in SSC profile of the different size fraction classes.
- Comparison of turbidity records derived from monitored rivers indicate that there is no standard conversion between turbidity values and quantitative mass measurements of the sediment as SSC.
- Various turbidity sensors exhibit different numerical responses, even when measuring sediment concentration within the same size fraction classes.
- Not only do different turbidity sensors exhibit distinct responses, but even similar turbidity sensors can yield different correlations in different rivers.
- In any specific river, turbidity sensors exhibit a robust linear correlation with sediment concentration.
- Comparing data derived from at-a-point ABS and turbidity sensors indicate a markedly strong correlation between ABS response and coarser suspended sediment (i.e., sand SSC). Turbidity sensors demonstrate a more robust correlation to silt and finer suspended sediments.
- At-a-point ABS (Acoustic Back Scatter) sensors significantly underestimate event load at monitoring sites where higher proportions of silt and finer fractions occur, compared to turbidity-derived loads.
- In flood events where sediment sampling occurred throughout the event, data derived from acoustic side-looking sensors provided more accurate sediment load estimates relative to at-a-point optical and acoustic sensors at all monitoring sites.

- At-a-point sensors are unable to accurately represent changes in sediment concentration throughout the cross-section, even when calibrated using cross-section averaged, discharge-weighted SSC.

The key findings derived from experience in setting up sensors and maintaining them in the field include:

- Installation of side-looking sensors is labour-intensive and expensive, because they need to be held in position with infrastructure that allows very little sensor movement under all flow conditions, ensuring that the acoustic path is maintained as close to horizontal across the river as possible, at all times. This is the primary installation drawback of the side-looking sensors when compared to at-a-point sensors.
- Side-looking ADCP instruments require relatively laminar flow and sufficient depth in a cross section. They should be installed in locations far from bridges or rough hydraulic features to minimise the impact of turbulent flow on measurements caused by these structures.
- Side-looking ADCP instruments require little maintenance other than periodic cleaning of the sensor faces when they can be accessed.
- At-a-point sensors generate small data volumes from a single timeseries compared with the large amount of data generated by side-looking ADCP sensors.
- Side-looking sensors can also provide estimates of flow at locations where the equipment used at standard stage discharge stations will not work.
- More data processing is required for side-looking ADCP sensors than for at-a-point sensors.

1 Introduction

1.1 Background

Sediment is one of the most pervasive and significant contaminants in New Zealand aquatic ecosystems. Suspended sediment (SS) has a major role in impairing water quality (e.g., through reduced visual clarity), degrading aquatic habitats (e.g., by smothering fish spawning habitat and estuarine shellfish beds), altering channel morphology, and creating operational issues in water supply facilities. Millions of dollars are spent in catchments to control erosion, but without accurate high-resolution (spatial and temporal) data for sediment loads, and information regarding the physical characteristics of the sediment being monitored, it is often unclear if this expenditure provides value for money and delivers the water quality outcomes required.

Mitigating the impact of sediment in fresh, estuarine and coastal waters requires accurate information on catchment suspended sediment concentration (SSC) and load. This has led to a growing regional council focus on high frequency, in situ suspended sediment monitoring, firstly to underpin regional erosion management initiatives but also to support catchment sediment load monitoring and limit setting under the National Policy Statement for Freshwater Management (NPS-FM 2020).

The NPS-FM (2020) directs councils to manage freshwater quality within limits; the Government's freshwater reforms (Ministry for the Environment and Ministry for Primary Industries 2018) proposed the introduction of sediment as a mandatory national attribute for ecosystem health for which limits must be set, monitored and reported on. Policy 4 of the NPS-FM (2020) stresses the requirement for integrated management, meaning that limits on sediment must be set, taking into consideration the effects of sediment on values associated with sensitive receiving environments such as lakes and estuaries. In the case of estuaries and other coastal environments, Policy 22 (sedimentation) of the New Zealand Coastal Policy Statement (NZCPS 2010) requires both monitoring and reduction of sediment loadings (as required), highlighting the need for robust and defensible techniques for quantifying catchment sediment loads. Information derived from these techniques is required for effective catchment management. In part it will direct where erosion mitigation is required (e.g., to reduce the impact of earthworks and other sediment generating activities). These procedures will also enable the efficacy of various mitigation measures to be quantified and indicate whether catchment load limits are being met.

A variety of technologies are now available for surrogate monitoring of SSC, including optical and acoustic back-scatter point-measurement or use of profiling instruments; some of these also provide particle size information. Even though operational experience and scientific trials have demonstrated that each of these technologies have practical limitations and that each technology provides different responses to varying suspended sediment characteristics (even within a given type of instrument – e.g., optical turbidity sensors), little guidance exists as to which surrogate technology is best suited for specific conditions, or how equipment may be operated most effectively. This is particularly important for acoustic instruments – although now commonly used in the United States for SS monitoring, these have seen relatively little use for this purpose in New Zealand. This is unfortunate, because side-looking Acoustic Doppler Current Profilers (ADCPs) are relatively widely used in New Zealand for monitoring stream velocity and discharge.

Side-looking ADCPs are primarily used to scan flow velocity across a stream channel by measuring the doppler shift of sound pulses scattered back off suspended particles. However, the intensity of the

sound back-scatter, once range-corrected, is a function of the suspended particle concentration, and so procedures have been developed to deconvolve this into an SSC record. This secondary functionality of ADCPs is little used in New Zealand but presents the opportunity to monitor SSC using existing instruments.

Continuous suspended sediment monitoring in New Zealand rivers has typically been done using turbidity (optical back-scatter, OBS) as a surrogate for SSC, but this has been fraught by issues such as sensor bio-fouling and reliability, range (many sensors in use saturate at moderately high SSCs during flood peaks, which is when suspended sediment loads are maximised), and a paucity of calibration of the at-a-point surrogate record to the cross-section average SSC. The lab-based cross-comparison of turbidity sensors built to the ISO7027 protocol (as specified in the New Zealand Turbidity Monitoring National Environmental Monitoring Standard (NEMS-Water Quality 2019)) undertaken by NIWA highlighted how instrument brands can respond differently when measuring natural sediment mixtures, even when calibrated to a reference “sediment” such as Formazin (Davies-Colley et al. 2021a; Davies-Colley et al. 2021b). Acoustic back-scatter (ABS) is an alternative SSC surrogate that avoids many of the issues with OBS instruments and can provide information on size grading if used with multiple frequencies.

1.2 Project brief

The “patchy” knowledge base regarding surrogate technologies for river suspended sediment load monitoring, along with some bad experiences (poor-quality data derived from previous turbidity sensor deployments), has discouraged investment in updated suspended sediment monitoring programs, including implementation of new technology. NIWA was commissioned by MBIE through the Envirolink scheme to provide guidance on the selection of appropriate surrogate monitoring technologies for robust measurement of the suspended sediment load to support freshwater and coastal management.

Regional Councils and Unitary authorities which are commencing, expanding, or rationalising suspended sediment monitoring programs, and which require time-series records of SSC to meet their monitoring and policy objectives, are the main audience of this report. Aimed primarily for use by Regional Councils and Unitary Authorities, this document will also be of use to external consultants who collect data and information associated with resource consent applications or monitoring. It is anticipated that the findings within this Envirolink Tools project will underpin the future development of a National Environmental Monitoring Standard (NEMS) for sediment monitoring.

To evaluate different surrogate technologies, multiple acoustic and optical instruments were deployed at different monitoring sites. The data, information and experience obtained from these deployments has been used (in part), to prepare this guidance.

1.3 Scope of the project

The aims of this project were to evaluate different suspended sediment surrogate monitoring technologies, including optical turbidity instruments and point and profiling acoustic back-scatter instruments. Criteria for evaluating and comparing each technology include:

- Procedures for data processing.
- Determining the accuracy and precision of estimates of SSC and suspended sediment loads determined from measurement of proxy variables.

- obtaining fit-for-purpose information for rivers having different sediment characteristics (e.g., sand vs mud-dominated, varying suspended sediment concentration ranges).
- Identifying and describing instrument installation requirements.

2 Data

Data and operational experience compiled at a network of four monitoring sites representing various New Zealand river types were used in this study. These monitoring sites were:

- Oreti River at Taramoa, Southland
- Mataura River at Mataura Island Bridge, Southland
- Grey River at Dobson, West Coast South Island
- Manawatu River at Teachers College, Manawatu-Whanganui¹

The rivers at all monitoring sites have a braided system. They change to a single thread river with a straight channel at the monitoring site. The selected monitoring sites cover a range of rivers draining catchments of varying size and lithologies. These variations will provide a more thorough assessment of sensors in different environments. Catchment area upstream of the monitoring sites together with the dominant landcover and dominant lithology are listed in Table 2-1.

Operation of this monitoring network was supported in part from NIWA Strategic Science Investment Fund (SSIF) – high frequency water quality monitoring research project, and in part by Horizons Regional Council. The NIWA SSIF project was specifically set up to provide the experience, data, and information required to underpin delivery of this Tools project. All the surrogate sensors used within this project were purchased using NIWA Strategic CAPEX funding.

2.1 Surrogate sensors

In general, three types of sediment surrogate sensors were used at these monitoring sites:

- Optical turbidity sensors (OBS).
- At-a-point acoustic backscatter (ABS) sensors.
- Side-looking (Horizontal) Acoustic Doppler Current Profilers (H-ADCPs).²

In-situ bank-mounted side-looking H-ADCPs were installed at all monitoring sites (Figure 2-1). These instruments can provide time-series estimates of SSC and sediment load whilst also providing a continuous record of channel velocity. The Teledyne ChannelMaster H-ADCP sensors and OTT side-looking doppler sensor (OTT-SLD) were used at some of these sites (see Table 2-1).

The optical turbidity sensors used in this study include:

- Observator Analite NEP-5000 used in the Oreti and Grey Rivers,
- Hach Solitax used in the Mataura River,
- A YSI EXO Turbidity Smart Sensor fitted to a YSI ExoSonde at the Manawatu River.

¹ For simplicity, from here we refer to the name of river as the name of monitoring site, for example; for the site Mataura River at Mataura Island Bridge, we use Mataura River

² They are also called Acoustic Backscatter Profilers (ABSPs)

All of these turbidity sensors are ISO 7027 compliant. Prior to their deployment in the field, all the sensors were calibrated against Formazin solutions, and as a result, the turbidity values were reported in Formazin Nephelometric Units (FNU).

The at-a-point ABS instrument used in this study is an 8 MHz Sequoia Scientific LISST-ABS sensor. The sensor comes factory calibrated to convert acoustic response into sediment concentration measurements. Therefore, the sensors give output in milligrams per litre (mg/L) or grams per cubic metre (g/m³), which corresponds to the unit used for sediment concentration measurement. The LISST-ABS data obtained from two monitoring rivers (i.e., Mataura and Manawatu Rivers) were used in this study.

In addition to the sediment data measurements, continuous flow records were measured at each site. Flow data were combined with sensor output to calculate sediment load.

Table 2-1: Characteristics of catchments upstream of the monitoring sites and a list of surrogate instruments used at each site.

.Sites (region)	Area (km ²)	Dominant landcover	Dominant lithology	Instruments (model)
Oreti River at Taramoa	2120	Pasture	Alluvial fans, Greywacke, Argilite and hard limestone	Turbidity sensor (Observer) H-ADCP (ChannelMaster 1200 kHz)
Mataura River at Mataura Island Bridge	3600	Pasture	Schist, Greywacke, Argilite and hard limestone	Turbidity sensor (Hach Solitax) ABS sensor (LISST-ABS) H-ADCP (ChannelMaster 1200 kHz)
Manawatu at River Teachers College	3900	Pasture	Hill country on sandstone, mudstone, and greywacke	Turbidity sensor (YSI EXO turbidity) ABS sensor (LISST-ABS) H-ADCP (OTT-LSD 1 MHz)
Grey River at Dobson	3830	Indigenous forest	Mixed lithology	Turbidity sensor (Observer) H-ADCP (ChannelMaster 1200 kHz)



Figure 2-1: Side-looking acoustic backscatter profilers deployed at the monitoring sites. Teledyne ChannelMaster was used at the Oreti, Mataura and Grey Rivers. OTT-SLD was used at the Manawatu River.

2.2 Sediment sampling

Sediment samples collected at each monitoring site include:

- at-a-point index SSC collected by autosamplers,
- manually gauged cross-section averaged SSC collected by isokinetic depth-integrated or point-integrated samplers.

During periods of flood events, discrete water samples were collected from each site using ISCO auto-samplers. Water samples collected with auto-samplers were used to establish the calibration relationship between surrogate measurements and at-a-point SSC.

Cross-channel sediment gaugings, along with automated water samples, were carried out during many of the high flow events in order to measure the cross-section average discharge-weighted SSC. For sediment gauging, different types of isokinetic depth-integrated suspended sediment samplers (e.g., D-49 and D-77) and point-integrated samplers (e.g., P-61) were used. The samplers were

deployed from NIWA jet boats (in the Maitava, Oreti, Grey Rivers), and from the Horizons Regional Council jet boat (in the Manawatu River).

The Equal Discharge Increment (EDI) method was used for the sediment gaugings. Five series of verticals, each representing equal increments of discharge, were sampled across the river at various times on the rising and falling stages of flood events.

Samples taken using both automated water samplers and sediment gauging samplers were analysed in the NIWA-Hamilton water quality laboratory for SSC. The samples were analysed to determine the SSC for two size fraction classes using a 63 µm sieve. We therefore had three SSC measurements for each sample:

- Silt and finer SSC (<63 µm)
- Sand and coarser SSC (>63 µm)
- Total SSC combining the two fractions.

Ad-hoc turbidity measurements were also made of the auto-samples in the laboratory. This was done to check for drift in the field sensor. The number of events and number of sediment samples collected for each site are listed in Table 2-2.

Oreti River: Over the time span from September 2017 to October 2020, a total of 265 autosamples were collected during 14 flood events. Of these flood events, four had simultaneous sediment gauging and autosampling results.

Maitava River: During a one-year period from June 2020, a total of 126 automated sediment samples were collected from seven flood events. Among these flood events, four had both concurrent auto-sample and sediment gauging samples, resulting in a total of 10 samples.

Manawatu River: The auto-samples were collected during nine flood events from June 2020 to November 2022. Among these flood events, two had both concurrent auto-sampling and sediment gauging. An event with a full coverage of the sediment samples in November 2022 was used to assess the performance of different surrogate sensors in estimating sediment load.

Grey River: Sediment samples were collected from four flood events between October 2020 and June 2023. This collection comprises a total of 79 auto-samples taken from the four flood events, along with seven sediment gauging samples acquired during two of those events.



Figure 2-2: Example of depth-integrated physical sampling in Oreti River . using a depth-integrated D77 sampler, which provides the direct measure of representative suspended sediment concentration in a river.

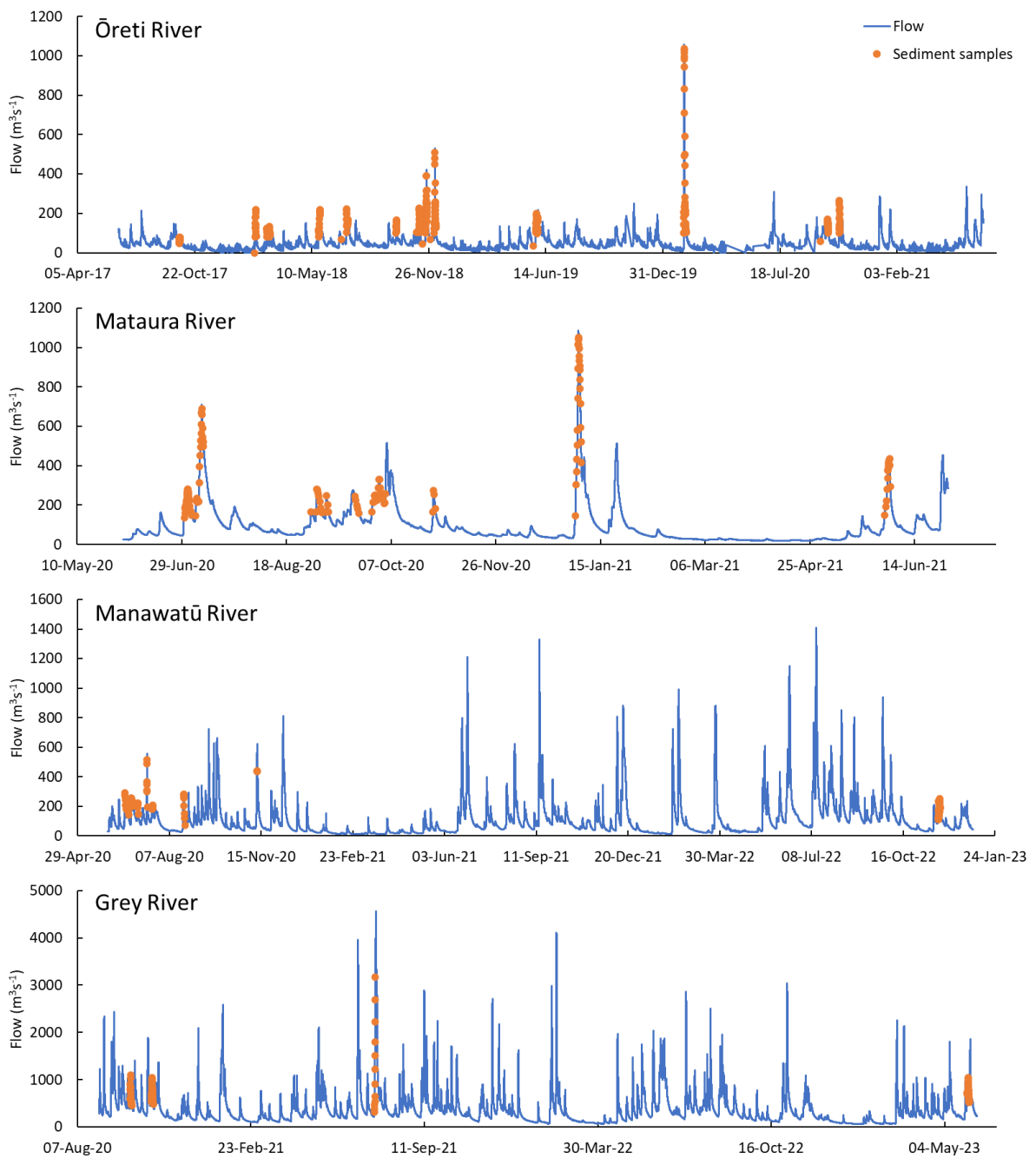


Figure 2-3: Continuous flow records and sediment samples used to calibrate the surrogate sensors at all monitoring rivers.

Table 2-2: Summary of collected suspended sediment samples and flow measurements at monitoring sites..

Site	No. of flood events with collected auto samples	Total no. of auto-samples collected*	No. of flood events with sediment gauging samples	Total no. of sediment gauging samples	Range of peak flows for sampled events (m ³ /s)
Oreti River	14	265	4	12	180 - 1100
Mataura River	7	126	4	10	240 - 1150
Manawatu River	9	75	2	6	210 - 600
Grey River	4	79	2	7	1050 - 4400

* the number of auto-samples used to calibrate the surrogate sensors vary for each sensor depending on the period of measurements for each sensor and data availability.

3 Analysis method

3.1 Approach

To evaluate the performance of surrogate sensors, the following approaches were used:

- Continuous surrogate records of the SSC were collected from all monitoring sites during high flow events. These include SSC measurements at an index point beside the bank, acquired through turbidity and at-a-point ABS sensors, as well as cross-sectional SSC measurements obtained using side-looking acoustic sensors.
- Calibrating at-a-point SSC data collected by autosamplers installed on the river bank to cross-section averaged SSC for different particle size classes, measured using depth-integrated and point-integrated samplers.
- Converting instantaneous surrogate records into cross section averaged SSC for different size fraction classes using derived relationships between surrogate measurements and cross-section averaged SSC (obtained in the previous step by calibrating at-a-point SSC to cross-section averaged SSC). Different regression relationships were used for each type of surrogate measurement technique and for each monitoring site (see Section 3.3 for further details on the calibration of turbidity sensors at each monitoring site, Section 3.4 for calibration of at-a-point ABS sensors, and Section 3.5 for calibration of side-looking acoustic sensors). These calibration relationships provide data that may be used to evaluate the effectiveness of the sensors in measuring SSC for different size fraction classes in rivers having different sediment characteristics.
- Calculate event sediment load for total SSC using physical measurements for events where continuous physical sediment measurements were available. Additionally, event sediment load for total SSC was determined from each surrogate sensor, and their respective results were compared against the measured sediment load to assess the performance of each sensor in estimating sediment load (see Sections 3.6 and 0).

3.2 At-a-point SSC measurements against cross-section averaged SSC

The calibration relationship between the at-a-point SSC, as collected by autosamplers, and the cross-section averaged discharge-weighted SSC, as collected by depth-integrated or point-integrated isokinetic samplers, was established for each site. With the utilization of these calibration relationships, it becomes possible to estimate the cross-section averaged SSC for all the samples collected by the autosampler. This in turn provides more robust data to evaluate surrogate sensors.

Linear regression with zero intercept was used for developing the relationships between at-a-point SSC measurements (SSCa) and cross section averaged (SSCg) for each size fraction classes:

$$SSCa = b \text{ SSCg} \quad (1)$$

Where b is the slope coefficient for the linear regression relationship.

3.3 Turbidity data measurements

A rigorous quality assurance procedure was employed to ensure reliable data from the turbidity sensor raw data records, before calibrating the records to SSC. The quality assurance included:

- **Removing unexpectedly high solitary data values (spikes).** Such spikes can occur due to electronic transients in the turbidity sensors or floating debris passing near the sensor's lens. Spikes were removed from the records by manual editing within the AQUARIUS software.
- **Adjusting bio-fouling ramps in turbidity records.** Bio-fouling occurs when objects enter and increasingly occupy the sensor's detection volume, leading to a steady increase in the sensor response over time. The primary cause is the growth of biofilms on the sensor's lens, particularly during the warmer summer months. Whenever such occurrences were detected, the raw turbidity records were ramp-adjusted, ensuring that the base turbidity level remained relatively constant throughout the recording period. To prevent biofouling in the first instance, it is essential to consistently inspect and clean the sensors. Employing mechanical wipers (or using other inhibitors as outlined in NEMS-Water Quality (2019)) can provide a continuous solution for inhibiting lens fouling.
- **Checking for turbidity sensor drift due to sensor aging.** Sensor drift occurs slowly with time. Turbidity sensor drift was checked by comparing the field and lab turbidity data to identify time trends in the normalised field-to-lab turbidity ratio.

All the turbidity records used in this study from all monitoring sites went through these assessment and data adjustment procedures. The corrected turbidity data resulting from these adjustments were then used in the calibration procedure. See Section 0 for the results of calibrating turbidity measurements to sediment concentration at each monitoring site.

3.4 At-a-point acoustic measurements

At-a-point ABS records from the LISST-ABS sensor were only available at two monitoring rivers with a good coverage of data: Mataura River and Manawatu River. Similar to the turbidity records, the raw ABS records from the LISST-ABS sensor were "cleaned" within the AQUARIUS software. Spikes in the data were removed through manual editing and by use of a numerical filter. ABS sensors are relatively less susceptible to signal degradation caused by biofouling, and during our study, no instances of biofouling were observed in the records from the two study sites. The corrected ABS data were then used in the calibration procedure. See Section 4.3 for the results of calibrating at-a-point ABS measurements to sediment concentration at Mataura and Manawatu Rivers.

3.5 Side-looking acoustic measurements

The principles of using acoustic profilers to obtain continuous record of SSC are well founded in theory (Landers et al. 2012; Topping et al. 2015; Wood et al. 2015) and these are now being applied in different rivers internationally, mostly by the United States Geological Survey – USGS (Landers et al. 2016; Topping and Wright 2016). To date however, there has been limited uptake and documented experience of use of acoustic technology (either as at-a-point sensors or side-looking acoustic back-scatter profilers ABSPs) for suspended sediment monitoring in New Zealand.

Advantages of acoustic suspended sediment measurement approaches over other sediment surrogate methods (notably turbidity) include:

- potential expansion of monitoring SSC at sites with existing ADCP instruments used in stream-flow velocity monitoring,

- being unaffected by changes in sediment colour compared to optical backscatter and turbidity measurements,
- ability to represent cross-section mean SSC compared to at-a-point surrogate instruments,
- retaining data integrity despite biofouling,
- providing information about the size grading of the suspended sediment load by using dual or tri-frequency acoustic profilers, and
- not requiring the intense cleaning that laser diffraction and optical instruments do.

To evaluate and compute acoustic surrogates, the surrogate analysis and index developer (SAID) standalone tool (Domanski et al. 2015), developed by the U.S. Geological Survey is used. This tool assists in the creation of ordinary least squares (OLS) linear regression models that relate constituent (e.g., suspended sediment concentration) and surrogate (i.e., side-looking acoustic measurements from different bin) parameters. The SAID tool assumes a spatially constant acoustic attenuation due to the presence of suspended particles. The SAID tool was developed using research that was done at the USGS by Topping et al. (2007); Wood and Teasdale (2013a); Wood et al. (2015).

The first step to build a linear model in SAID tool is to synchronize observations from the surrogate datasets (i.e., acoustic measurements) to observations from the constituent dataset (i.e., SSC measurements). The date and time of the constituent dataset are matched with the date and time of surrogate measurement. The matched dataset is then used to develop the linear model.

After matching the variables in time, the sediment corrected backscatter can be determined by converting measured backscatter to water corrected backscatter and finally to sediment corrected backscatter. The calculation of these parameters is described by Landers et al. (2016).

The formats that should be used to enter both acoustic data from the ADCP measurements and SSC data from the physical sample measurements for subsequent use in the SAID tool are explained in Appendix A.

The sediment acoustic rating curve will be developed using ordinary least squares linear regression. The model takes the form of:

$$\log_{10} SSC = b_0 + b_1 SCB$$

Where intercept (b_0) and slope (b_1) coefficients were determined using correlation between observed SSC and measured SCB. Previous studies found some estimates for these coefficients. Wright et al. (2010) found that b_1 should have positive values, with theoretical values of approximately 0.1. Other recent USGS studies (Wall et al. 2006; Wood and Teasdale 2013b; Medalie et al. 2014) found that the slope coefficient for SSC range between 0.03 and 0.1. The b_0 coefficient (intercept) may be either positive or negative but must not be forced to equal zero since the regression relationship may not represent the best fit to the observed data.

Scatter plots should be used together with coefficients of determination (R^2), and root mean squared error (RMSE) to evaluate the reliability and linearity of relations between SSC and acoustic explanatory variable.

After developing the regression relationship between SSC and sediment-corrected backscatter, the SSC can be predicted for ungauged acoustic measurements using retransformation of the regression model:

$$SSC = 10^{(b_0 + b_1 SCB)} \times BCF$$

Where BCF is bias-correction factor. The BCF accounts for transformation bias and is defined as:

$$BCF = \frac{\sum_{i=1}^n 10^{(Obs_i - Pred_i)}}{n}$$

Where n represents the number of observations, Obs is log₁₀ transformed observed SSC, and Pred is SSC calculated using regression equation. BCF values typically range between 1.01 to 1.1 for regression of log-transformed SSC on SCB. A plot of residuals between observed and predicted SSC against fitted values can also be used to determine if residuals have a variance that is constant with the explanatory variable.

3.6 Evaluating performance of the surrogate sensors in estimating sediment load

In order to assess the performance of different surrogate sensors in estimating sediment load, flood events were carefully chosen at each monitoring site, ensuring a continuous collection of physical samples throughout the event. To minimize uncertainties arising from cross-sectional variation in the SSC, and ultimately in the surrogate-derived sediment load estimates, events were specifically selected where both the continuous SSC derived from autosamples and cross-section-averaged discharge-weighted SSC were measured. Selected events from each monitoring site are listed in Section 5.4.

To establish continuous records of SSC, instantaneous acoustic and optical surrogate measurements were converted into cross-section averaged SSC values through a two-step calibration process:

- i) By calibrating surrogate records against autosampled SSC, the at-a-point SSC values were determined (see Sections 3.3 to 3.5).
- ii) Additionally, surrogate records were calibrated against sediment gauging measurements to determine cross-section averaged SSC values (see Section 3.2).

Subsequently, the event load (in t) was calculated by multiplying the surrogate-derived SSC with the flow rate (Q) for each time step (dt) after adjusting for unit conversions, and then summing these values over the entire duration of the flood event, from beginning to end (t_{start} to t_{end}):

$$Event\ load = \int_{t_{start}}^{t_{end}} SSC_t Q_t dt \quad (2)$$

Similarly, to determine “measured” sediment load, the SSC obtained from physical samples (i.e., at-a-point SSC from autosamples calibrated to cross-section averaged SSC from sediment gauging) was multiplied by the corresponding flow rate and sampling time intervals, using Equation (2).

To compare the accuracy of load estimates derived from different sensors, the relative error was calculated:

$$Relative\ Error = (surrogate\ derived\ load - measured\ load) / measured\ load \quad (3)$$

Assessments for each monitoring site and example events are listed in Section 0.

4 Results

4.1 The results of calibrating at-a-point SSC to cross-section averaged SSC

Oreti River (Figure 4-1): A robust correlation was observed between the auto-sampled SSC (SSCa) and the gauged SSC (SSCg) for total SSC ($R^2=0.99$) and silt SSC ($R^2=0.99$). However, the correlation was weak for sand SSC ($R^2= 0.69$). Given that sand constitutes a minor fraction of the gauged sediment samples in the Oreti River (falling within the range of 2% to 17% of the total SSC), their limited correlation does not significantly affect the relationship between auto-sampled and gauged cross-section average total SSC (which is a combination of the silt and sand SSC). The slope coefficient on the SSCg vs SSCa linear regression was remarkably higher for sand fraction, likely due to the higher concentration of sand and coarser suspended particles near the riverbed and in deeper sections of the river. These areas of the river channel are not adequately sampled by autosamplers positioned at the riverbank.

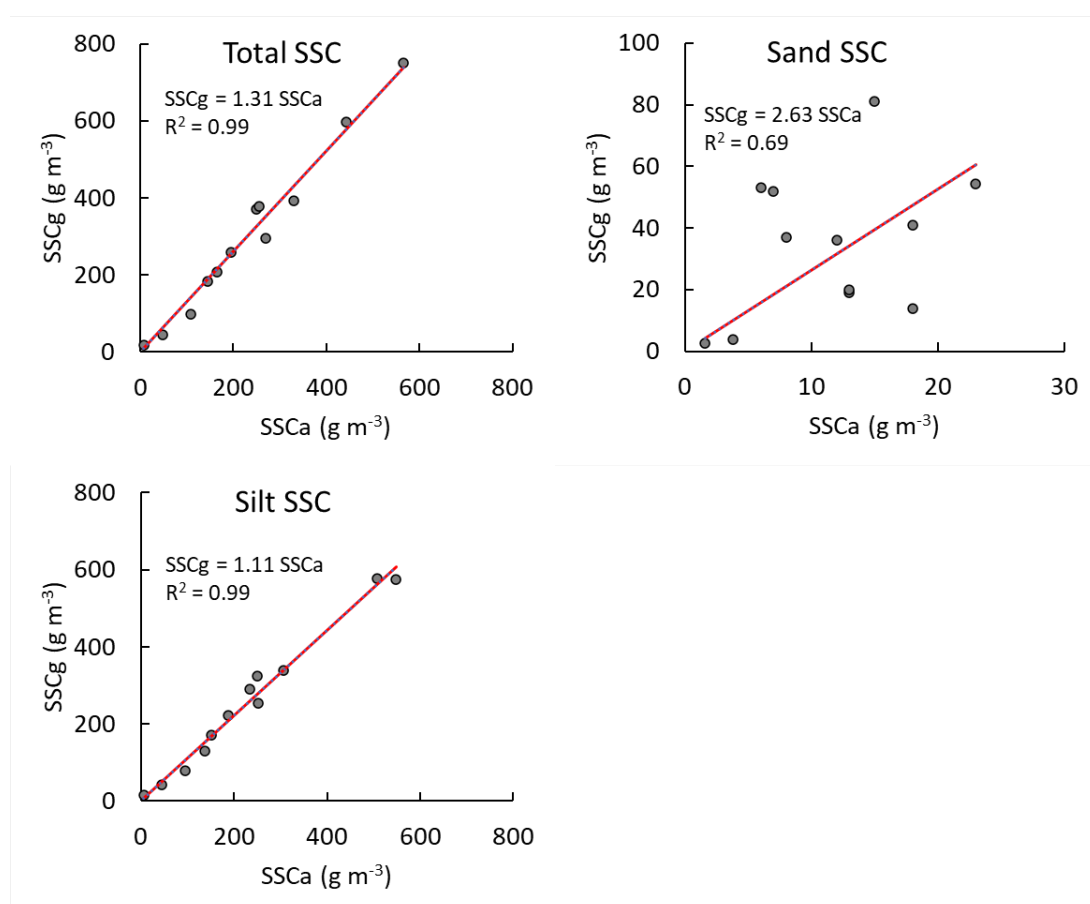


Figure 4-1: Relationship between auto-sampled and gauged cross-section . average SSC for three size fraction classes: silt and finer, sand, and total SSC at the Oreti River.

Mataura River (Figure 4-2): SSCg exhibited a strong association with SSCa for all three size classes, as evidenced by R-squared values exceeding 0.8. Similar to the Oreti River, the regression coefficient was higher for the sand fraction (1.45) in comparison with the total (1.15) and the silt (0.82) SSC.

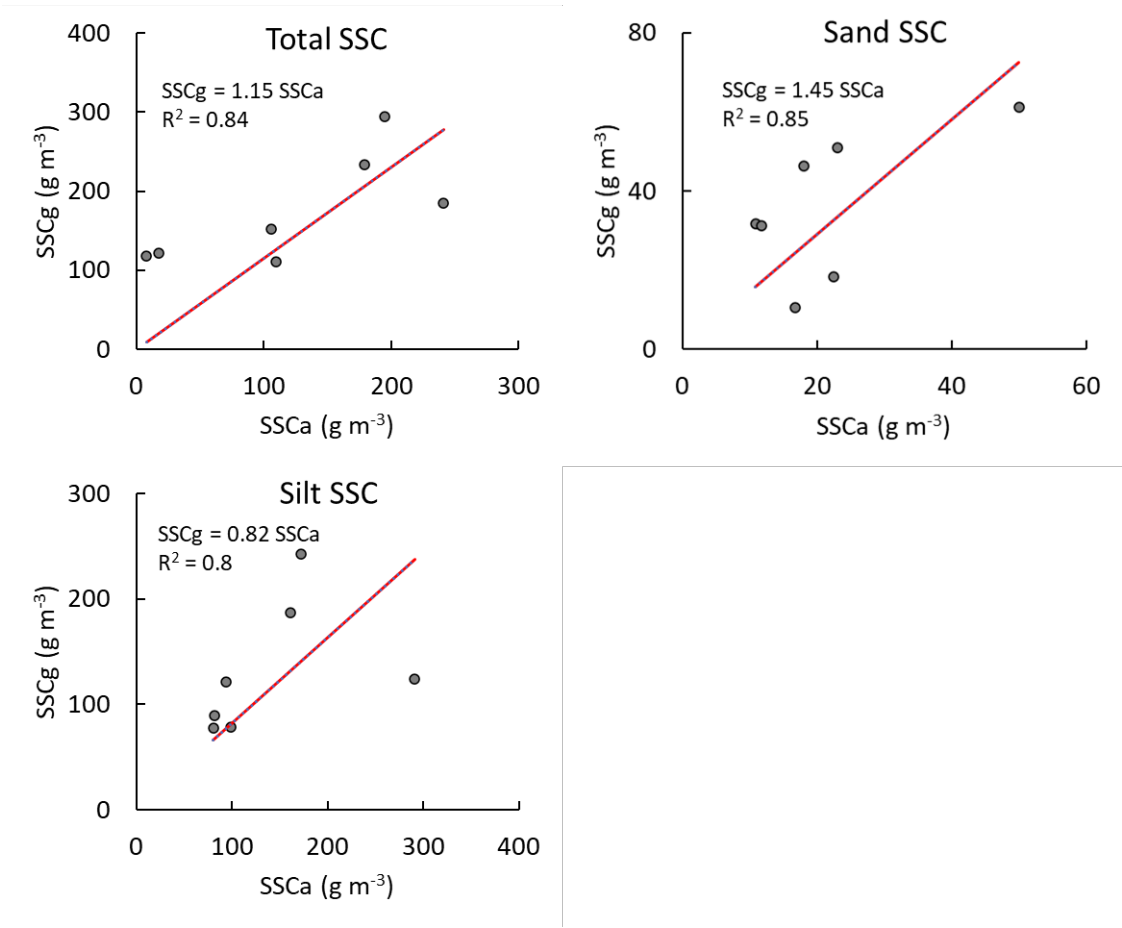


Figure 4-2: Relationship between auto-sampled and gauged cross-section average SSC for three size fraction classes. silt and finer, sand, and total SSC at the Mataura River.

Manawatu River (Figure 4-5): The SSCg was highly correlated with the SSCa across all three size fraction classes, with an R-squared value exceeding 0.99. The regression coefficients indicate that the sediment concentration throughout the river cross section at the monitoring site was 7% higher for the total SSC and 2% higher for the silt SSC compared to the sediment concentration measured using an autosampler at a river bank. Notably, the river cross-section sand exhibited a significantly higher SSC compared to the autosampled SSC (29% higher).

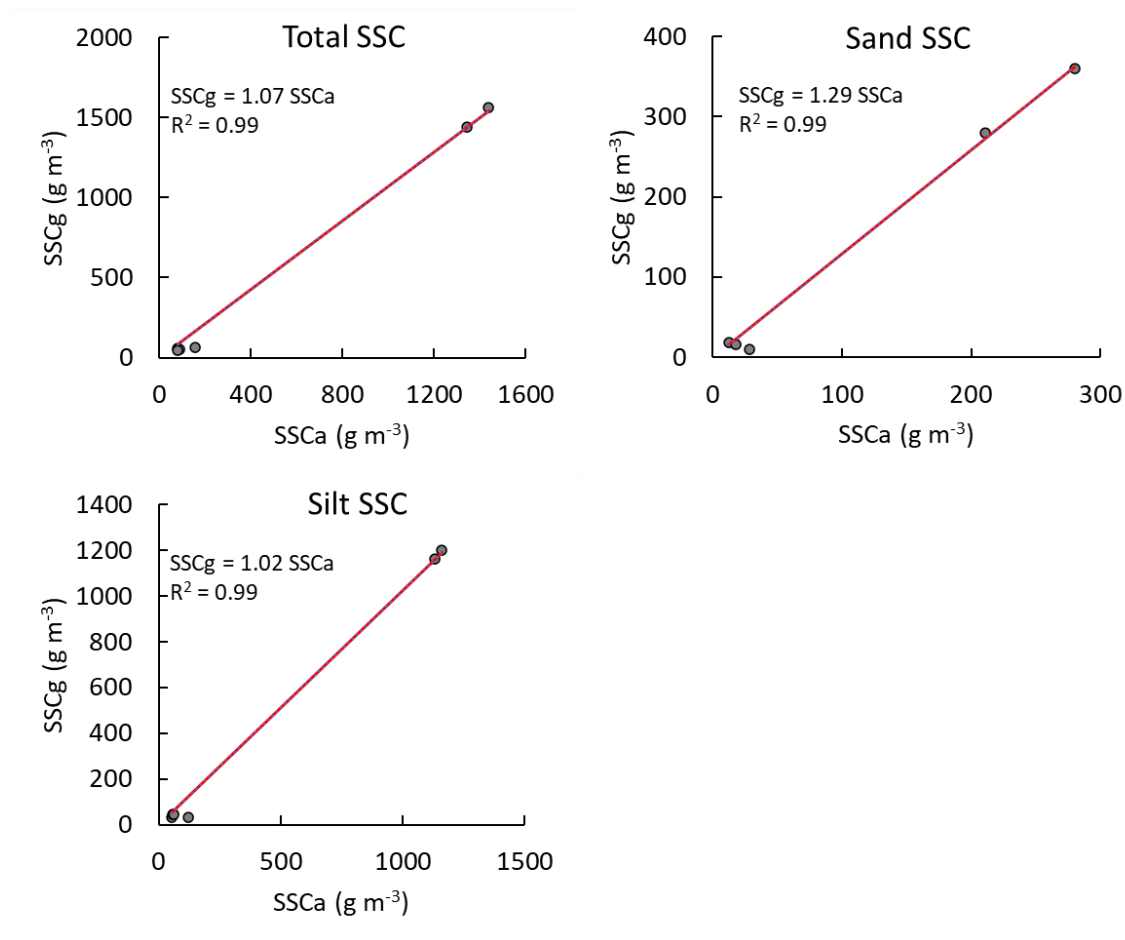


Figure 4-3: Relationship between auto-sampled and gauged cross-section average SSC for three size fraction classes. silt and finer, sand, and total SSC at the Manawatu River.

Grey River (Figure 4-7): The SSCg was highly correlated with the SSCa in all three size fraction classes, with R-squared values ranging from 0.83 for the sand SSC to 0.98 for the silt SSC. In contrast to the three other sites, the regression coefficient for the Grey River was less than one across three size fraction classes, with coefficients ranging from 0.64 for the sand SSC to 0.92 for the silt SSC. This is mainly because the autosampler sampling tube in the Grey River was installed within a riverbank section characterised by greater depth and higher flows.

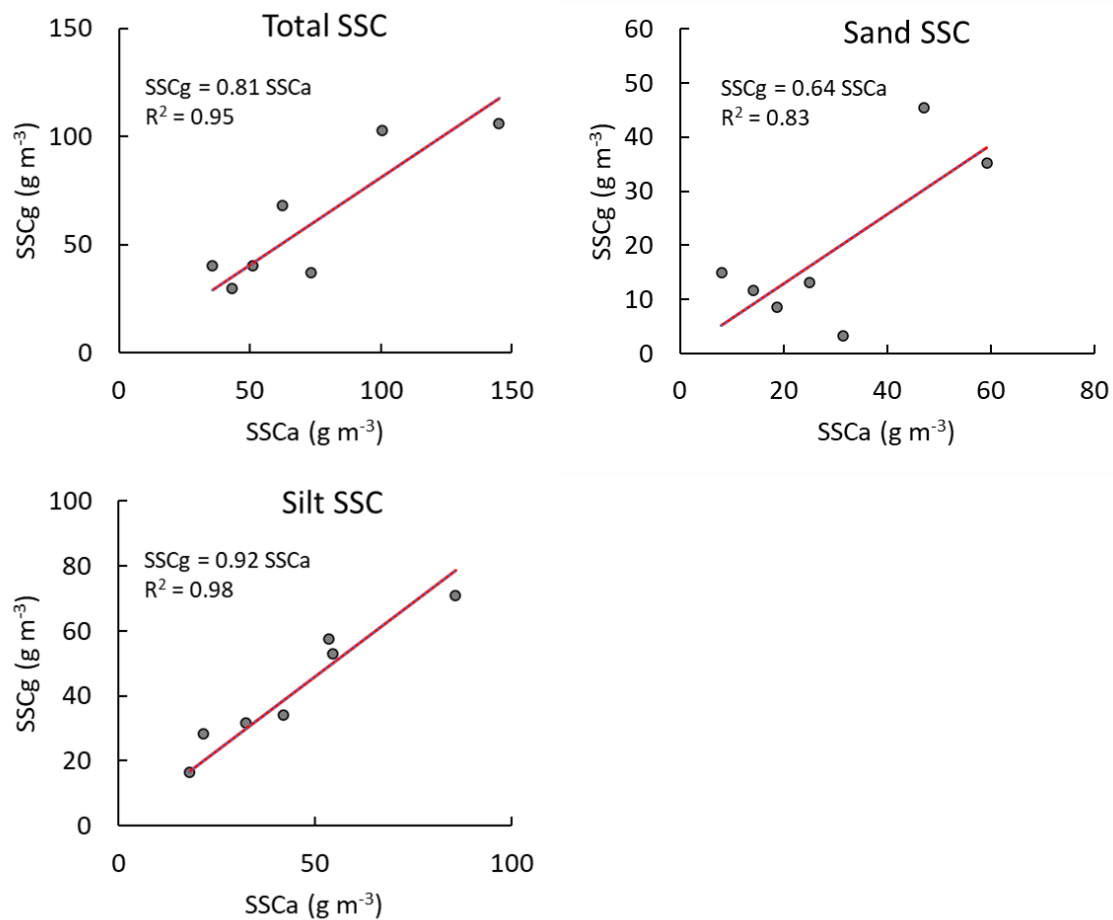


Figure 4-4: Relationship between auto-sampled and gauged cross-section average SSC for three size fraction classes: silt and finer, sand and total SSC at the Grey River.

4.2 The results of calibrating turbidity measurements

After cleaning the turbidity records based on the procedure summarised in Section 3.3, a correlation relationship was developed between corrected field turbidity records and autosampled sediment concentration for the three size fraction classes: sand SSC, silt SSC and the sum of both – total SSC. The linear regression with zero intercept was used to relate turbidity and SSC records.

Oreti River (Figure 4-8): There was a strong correlation between the field turbidity records and auto-sampled sediment concentration for both the silt SSC and the total SSC both with R-squared of 0.97. The turbidity measurements against sand SSC were widely scattered with R-squared of 0.6. This shows the poor response of the optical sensors against coarser particles.

Mataura River (Figure 4-9): A robust correlation was observed between the turbidity records and autosampled SSC for both total and silt size fractions, with R-squared of 0.98. As expected and similar to the Oreti River, the turbidity responses were not highly correlated against autosampled SSC.

Manawatu River (Figure 4-10): The silt SSC had best correlation with turbidity with an R-squared of 0.94 and a standard error (SE) of 89.6 g m^{-3} , followed by the total SSC ($R^2 = 0.89$, $SE = 220 \text{ g m}^{-3}$). The sand fraction of sediment, however, was poorly correlated against turbidity measurements ($R^2 = 0.56$, $SE = 224 \text{ g m}^{-3}$).

Grey River (Figure 4-11): In line with the other rivers, both the silt SSC ($R^2 = 0.98$, $SE = 9.4 \text{ g m}^{-3}$) and total SSC ($R^2 = 0.91$, $SE = 45 \text{ g m}^{-3}$) displayed strong correlations with the turbidity measurements. However, the relationship with sand was more scattered ($R^2 = 0.81$, $SE = 12 \text{ g m}^{-3}$).

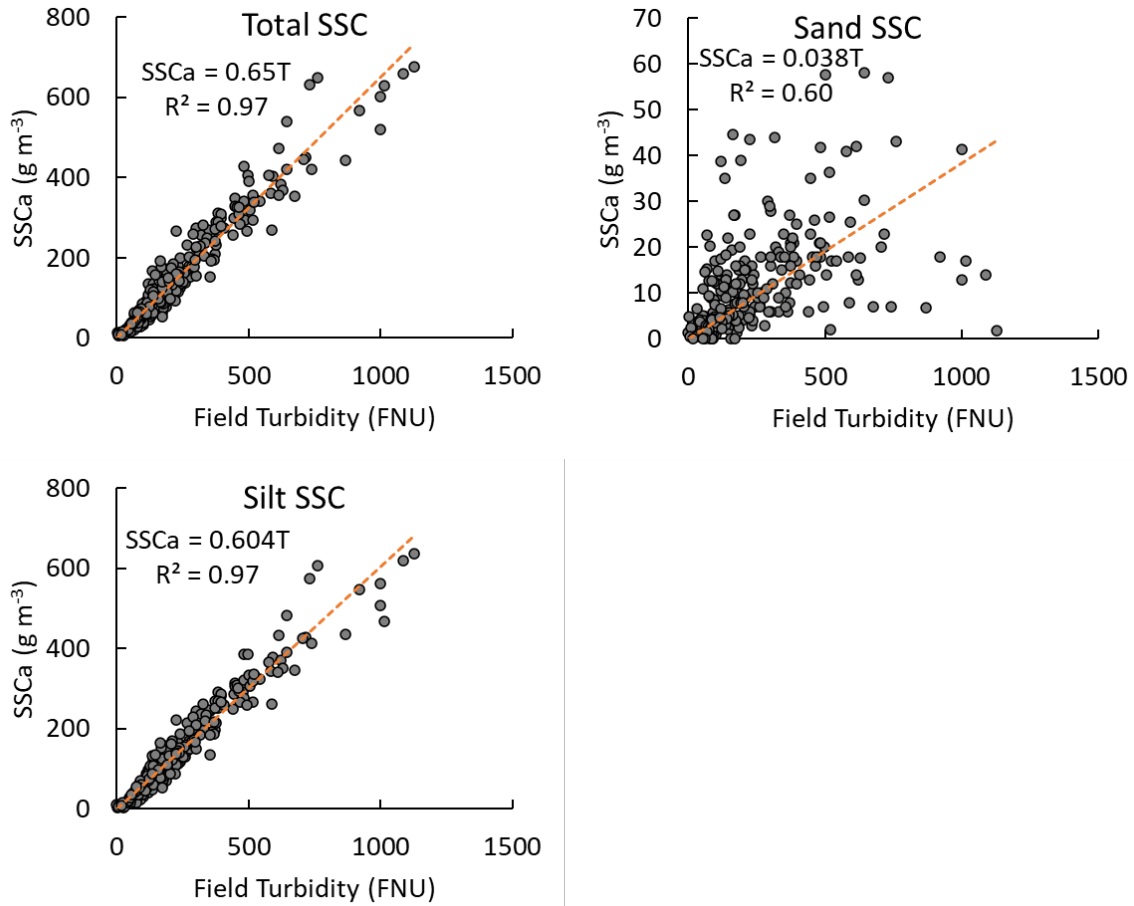


Figure 4-5: Relationship between auto-sampled SSC and field turbidity for three size fraction classes: silt and finer, sand, and total SSC at the Oreti River.

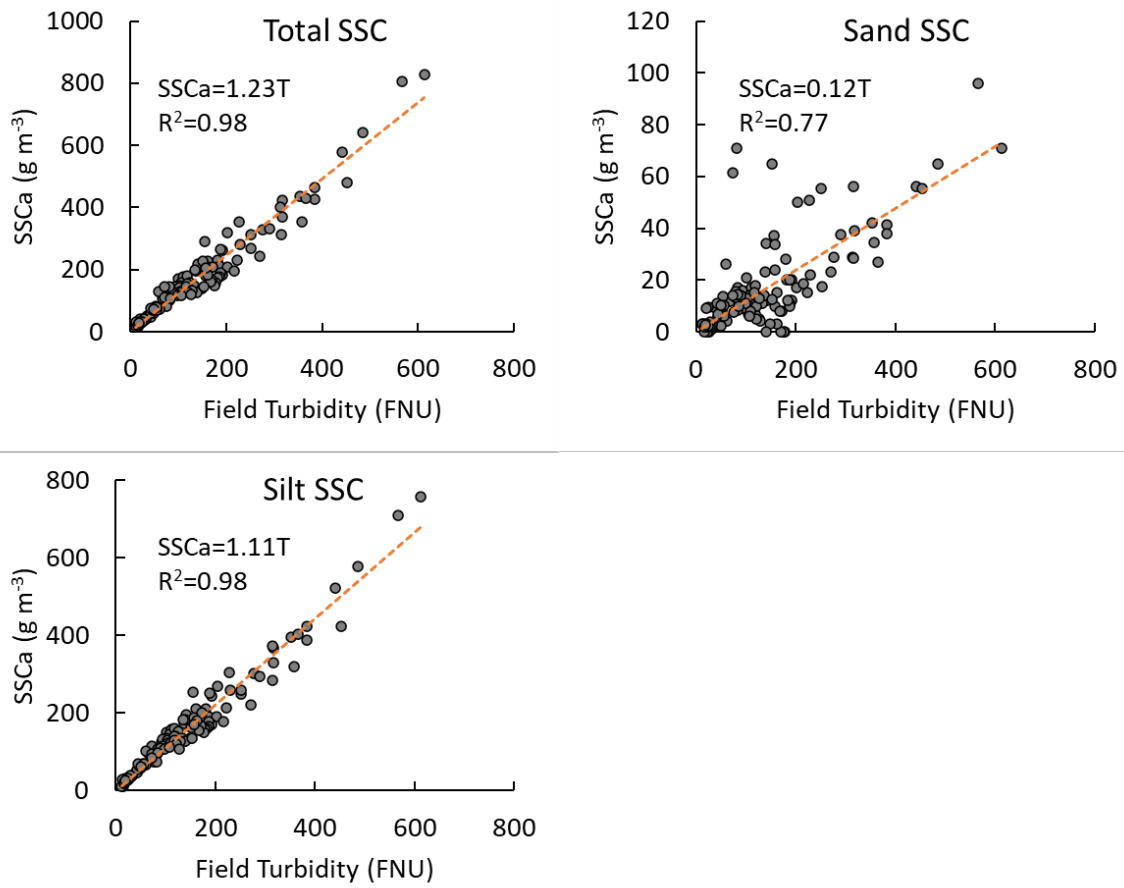


Figure 4-6: Relationship between auto-sampled SSC and field turbidity for three size fraction classes: silt and finer, sand, and total SSC at the Mataura River.

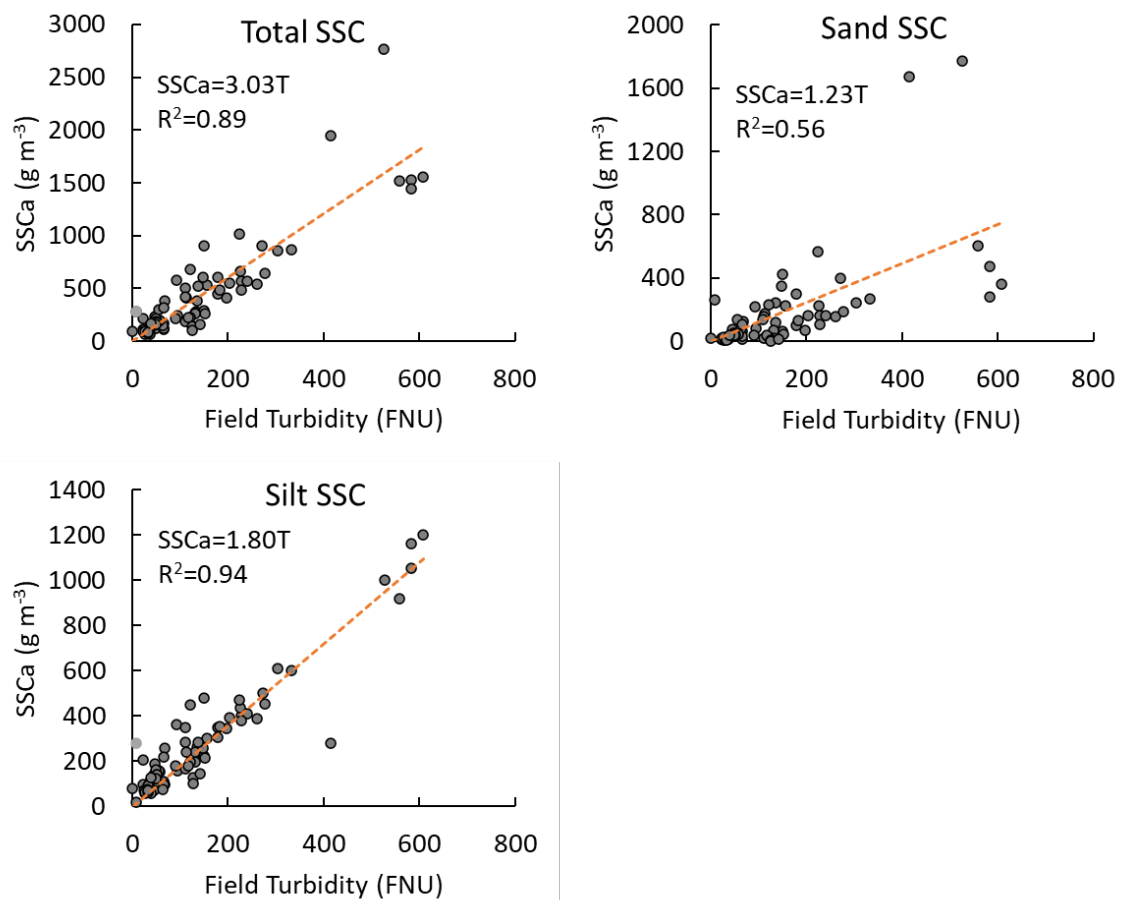


Figure 4-7: Relationship between auto-sampled SSC and field turbidity for three size fraction classes: silt and finer, sand, and total SSC at the Manawatu River.

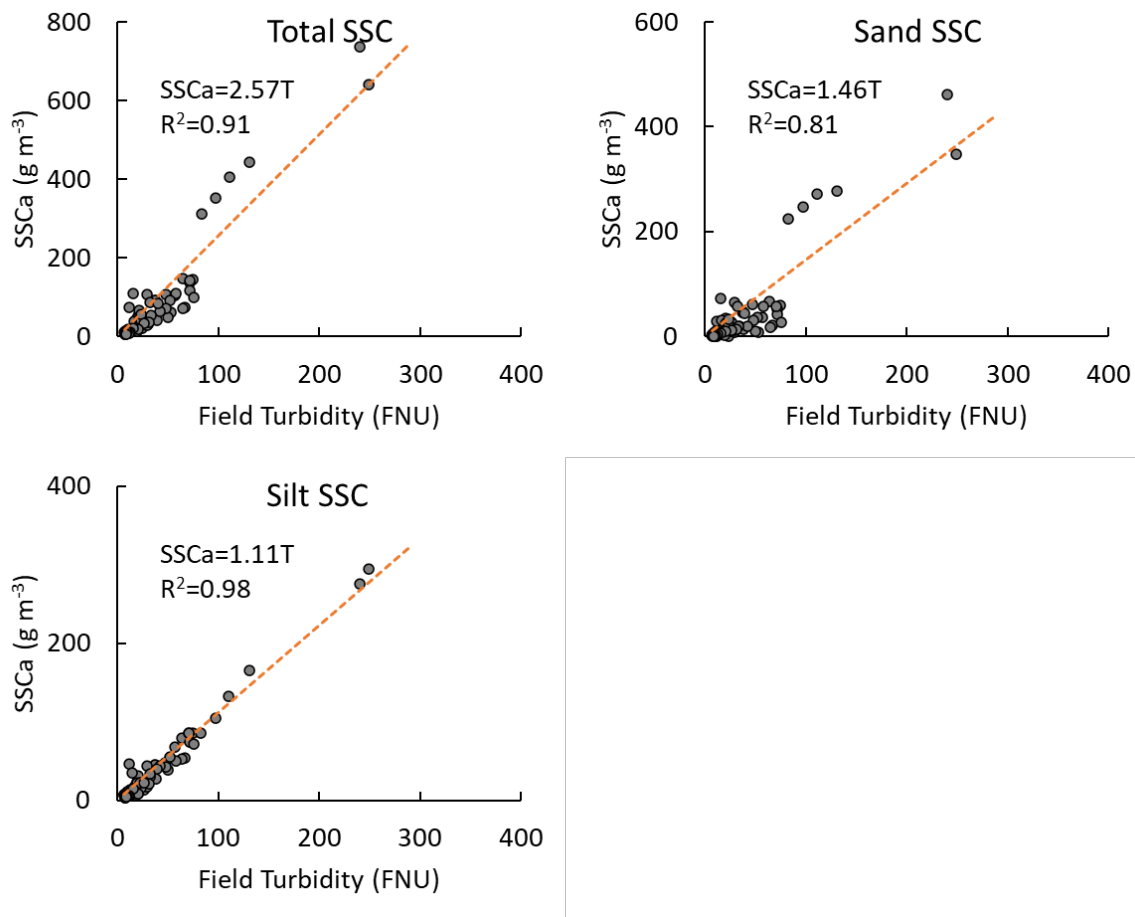


Figure 4-8: Relationship between auto-sampled SSC and field turbidity for three size fraction classes: silt and finer, sand, and total SSC at the Grey River.

Although all the turbidity sensors had linear regression relationships between turbidity and SSC (listed in Table 4-1), the regression coefficients varied between sites (for same size fraction classes). These variations in the relationships between sites may be attributed to inherent differences between the turbidity sensors, as well as the variability in sediment characteristics, including size mixture, colour, mineral content, and organic composition (Haddadchi and Hicks 2020). Regarding turbidity sensor variability, previous studies by Rymaszewicz et al. (2017) and Davies-Colley et al. (2021a) tested different turbidity sensors against known pre-prepared identical sediment concentrations. Their findings revealed that, despite calibration to a Formazin standard, the sensor responses to identical sediment concentrations varied considerably. While such sensor differences may pose challenges when turbidity itself is the primary property of interest, they should not be problematic when the sensors are used as surrogate for SSC measurement, provided separate calibrations are determined for each sensor and site, as was the case in this study.

Table 4-1: Regression characteristics and uncertainties in relationship between auto-sampled SSC and turbidity for all monitoring sites.

Sites	Total SSC			Sand SSC			Silt SSC		
	b-coefficient	R ²	Standard Error (g/m ³)	b-coefficient	R ²	Standard Error (g/m ³)	b-coefficient	R ²	Standard Error (g/m ³)
Oreti River	0.65	0.97	36.2	0.04	0.6	10.2	0.6	0.97	31.6
Mataura River	1.23	0.98	34.4	0.12	0.77	12	1.11	0.98	27.9
Manawatu River	3.03	0.89	220.5	1.23	0.55	224.2	1.8	0.94	89.6
Grey River	2.57	0.91	44.8	1.46	0.81	12.2	1.11	0.98	9.4

4.3 The results of calibrating at-a-point ABS measurements

Mataura River (Figure 4-10, Table 4-4): In contrast to the turbidity sensor, the sand SSC had a strong relationship against the point ABS records with R-squared of 0.94 and standard error of 5.5 g m⁻³ (compared to the turbidity sensor's R-squared of 0.77 and SE of 12 g m⁻³). However, the silt SSC had a weaker relationship against ABS records (R²=0.9, SE = 61 g m⁻³) in comparison to the turbidity sensor (R²=0.98, SE = 28 g m⁻³). Considering that the samples collected from the Mataura River contain significantly higher silt concentrations than sand, the former exerts a more substantial influence on the relationship between the total SSC and surrogate measurements. Consequently, the total SSC shows a stronger correlation with the turbidity (R²=0.98, SE = 34 g m⁻³) than with the point ABS (R²=0.92, SE = 63 g m⁻³).

Manawatu River (Figure 4-13, Table 4-4): As for the Mataura River, the point ABS provided stronger response to the coarser sediment particles (i.e., sand SSC R²=0.81, SE = 148 g m⁻³) than to the finer materials (i.e., silt SSC R²=0.7, SE = 207 g m⁻³).

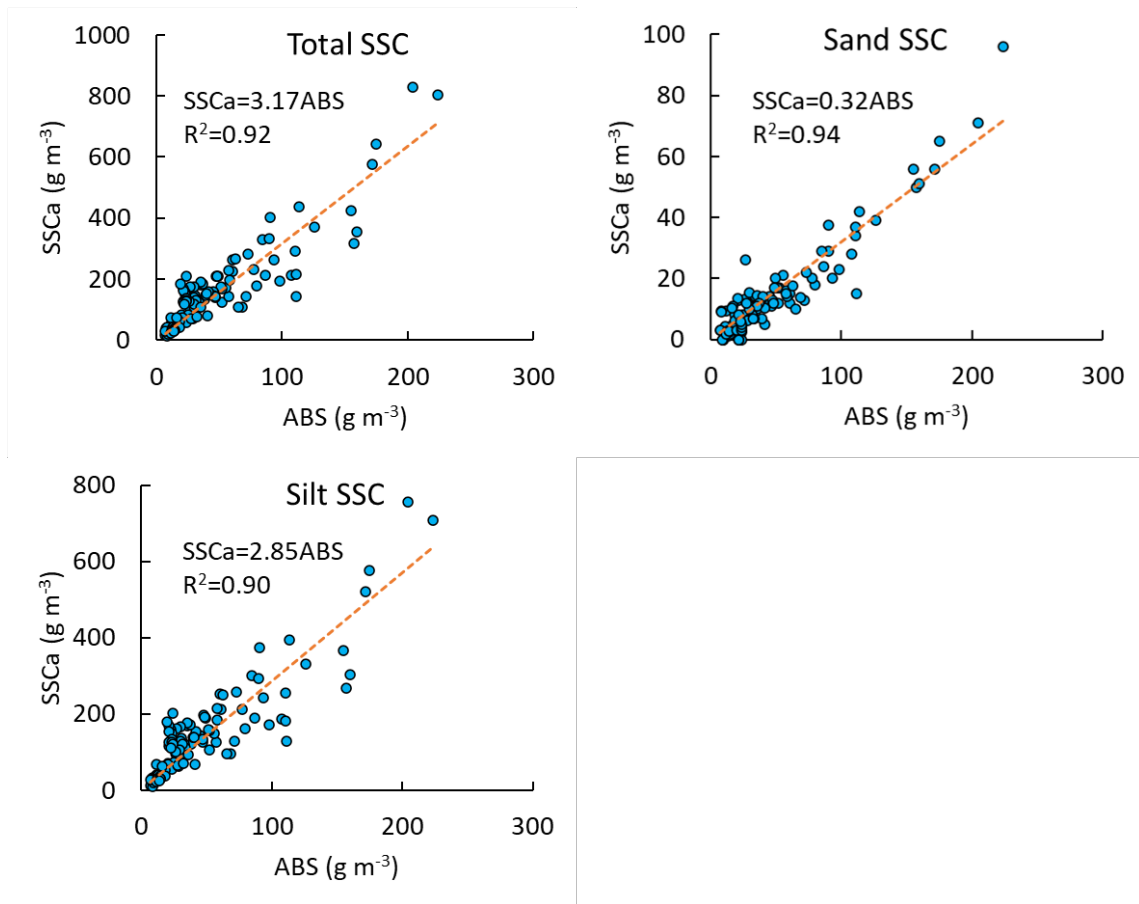


Figure 4-9: Relationship between auto-sampled SSC and at-a-point acoustic measurements for three size fraction classes: . silt and finer, sand, and total SSC at the Mataura River.

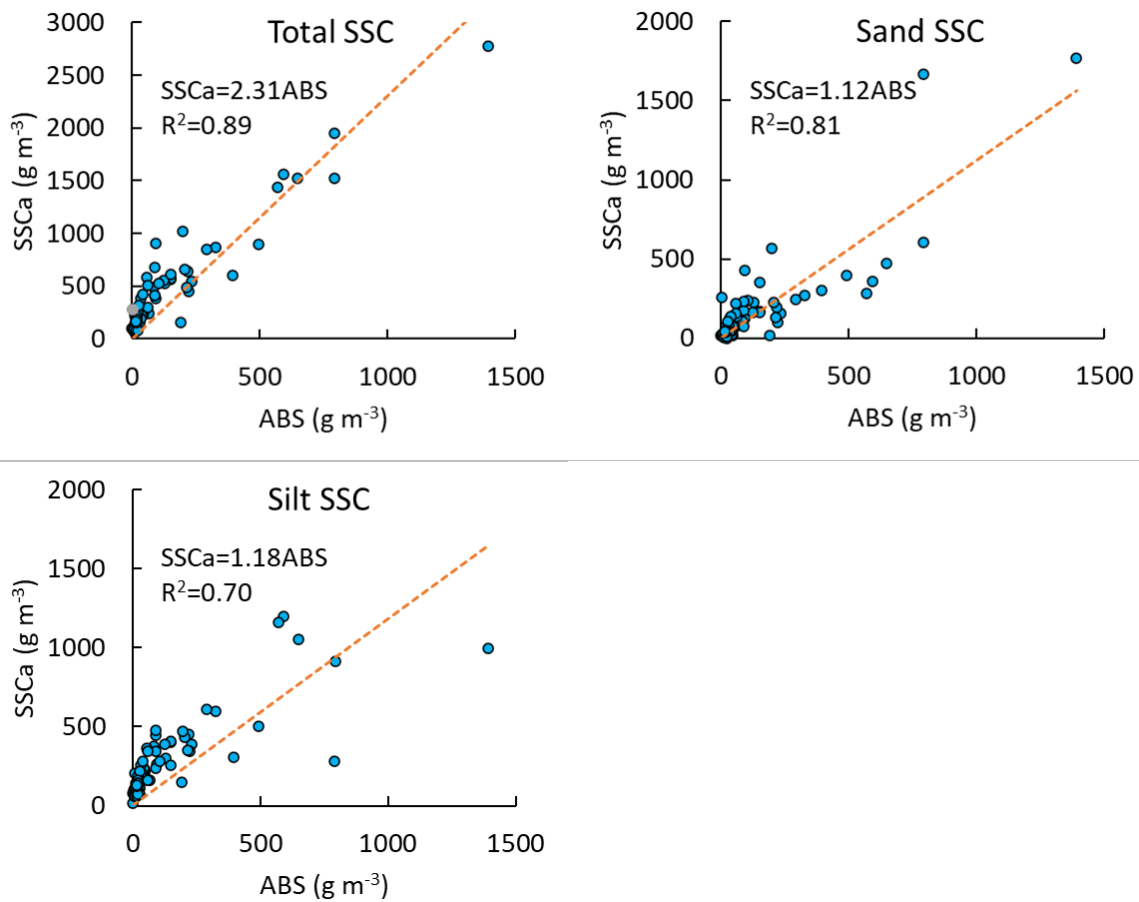


Figure 4-10: Relationship between auto-sampled SSC and at-a-point acoustic measurements for three size fraction classes: silt and finer, sand, and total SSC at the Manawatu River.

Table 4-2: Regression characteristics and uncertainties in relationship between auto-sampled SSC and at-a-point acoustic (LISST-ABS) for Mataura River and Manawatu River.

Sites	Total SSC			Sand SSC			Silt SSC		
	b-coefficient	R ²	Standard Error (g/m ³)	b-coefficient	R ²	Standard Error (g/m ³)	b-coefficient	R ²	Standard Error (g/m ³)
Mataura River	3.17	0.92	62.7	0.32	0.94	5.5	2.85	0.9	61.1
Manawatu River	2.31	0.89	219.3	1.12	0.81	147.9	1.18	0.70	207.3

4.4 Calibration of side-looking acoustic data using SAID toolbox

The SAID toolbox computes the sediment attenuation coefficient and sediment corrected backscatter from ADCP acoustic measurements.

After inserting input data, the SAID model will match acoustic measurements and SSC datasets by finding the minimum absolute difference between the times of observation of the constituent and surrogate data. The maximum time difference of 15 minutes was used for matching these variables in all monitoring sites.

A series of configuration and processing parameters are required by SAID to process acoustic backscatter data. Configuration and processing parameters of ADCP sensors deployed on each site is listed in Table 4-3.

Table 4-3: Configuration and processing parameters to calculate acoustic surrogates. Amp = backscatter counts, SNR = signal-to-noise ratio.

Parameter selection	Mataura at Island Br 1200 kHz	Oreti at Taramoa	Manawatu at Teachers College	Grey at Dobson
Configuration parameters				
Frequency (kHz)	1200	1200	1500	1200
Effective Transducer Diameter (m)	0.0507	0.0507	0.025	0.0507
Beam Orientation	Horizontal	Horizontal	Horizontal	Horizontal
Slant Angle (deg)	20	20	2.3	20
Blanking distance (m)	2	1	0.5	3
Cell Size (m)	1	0.7	2	1
Number of Cells	28	20	9	25
Processing parameters				
Moving average span	1	1	1	1
Backscatter values (Amp or SNR)	Amp	Amp	Amp	Amp
Intensity Scale Factor	0.41	0.39	0.5	0.4
Minimum Cell Mid-Point Distance (m)	2.58	1.41		4.58
Maximum Cell Mid-Point Distance (m)	10.58	11.91		12.58
Minimum number of cells	5	5	5	5
Near field correction?	No	No	No	No
Water Corrected Backscatter (WCB) profile adjustment	Yes	Yes	Yes	Yes

Oreti River: ADCP data were collected starting from 9 May 2019. A total of 69 sediment concentration data points (measured by autosamplers and calibrated to cross-section averaged SSC, as explained in Section 3.2) were aligned with acoustic data obtained from the ChannelMaster 1200 kHz instrument. The relationship between measured backscatter, water corrected backscatter, and sediment corrected scatter (SCB) (all in decibel units) against the cell mid-point cross-sectional distance along the acoustic beam for matched measurements in the Oreti River are shown in Figure 4-11.

An ordinary least squares linear regression model was developed in the SAID toolbox using the sediment corrected backscatter and log-transformed SSC datasets. The model demonstrates a strong agreement between logarithmic total SSC and sediment corrected backscatter measurements with an R-squared value of 0.91, a root-mean squared error of 109 g m^{-3} , and a bias correction factor of 1.14 (Figure 4-12, Table 4-4). A linear model with an intercept of -4.5 and a slope of 0.08 were used to estimate continuous total SSC records for the time periods of interest.

Mataura River: ADCP data collected starting from 20 February 2019. A total of 99 sediment samples were aligned with the acoustic records obtained from the ChannelMaster 1200 kHz instrument. The backscatter profiles for the aligned measurements are shown in Figure A-3 (Appendix A). In these aligned measurements, the sediment corrected backscatter ranged from 88 to 99 dB. Using the linear regression model, the mean sediment corrected backscatter measurements showed good agreement with the log-transformed SSC, as evidenced by an R-squared value of 0.81, root-mean squared error of 58 g m^{-3} , and a bias correction factor of 1.06 (Figure 4-12, Table 4-4).

Manawatu River: A total of 42 sediment samples were aligned with the ADCP data collected by the OTT-LSD 1.5 MHz instrument since its installation on 12 July 2019. During the times of sediment sampling, sediment corrected backscatter ranged from 91 to 108 dB. The regression model showed reasonable agreement between log-transformed SSC and the mean sediment corrected back scatter, as indicated by an R-squared value of 0.81, a root-mean squared error of 190 g m^{-3} , and a bias correction factor of 1.04 (Figure 4-12, Table 4-4).

Grey River: The ADCP data collected by the ChannelMaster 1200 kHz instrument, which was operating at the site since 15 March 2019, was matched with grab sediment samples. The ADCP data ranged from 87 to 115 dB at the time of sampling (Figure A-5). Using the linear regression model, mean sediment corrected backscatter measurements had a good agreement with the log-transformed SSC with R-squared of 0.81, root-mean squared error of 79.4 g m^{-3} , and bias correction factor of 1.07 (Figure 4-12, Table 4-4).

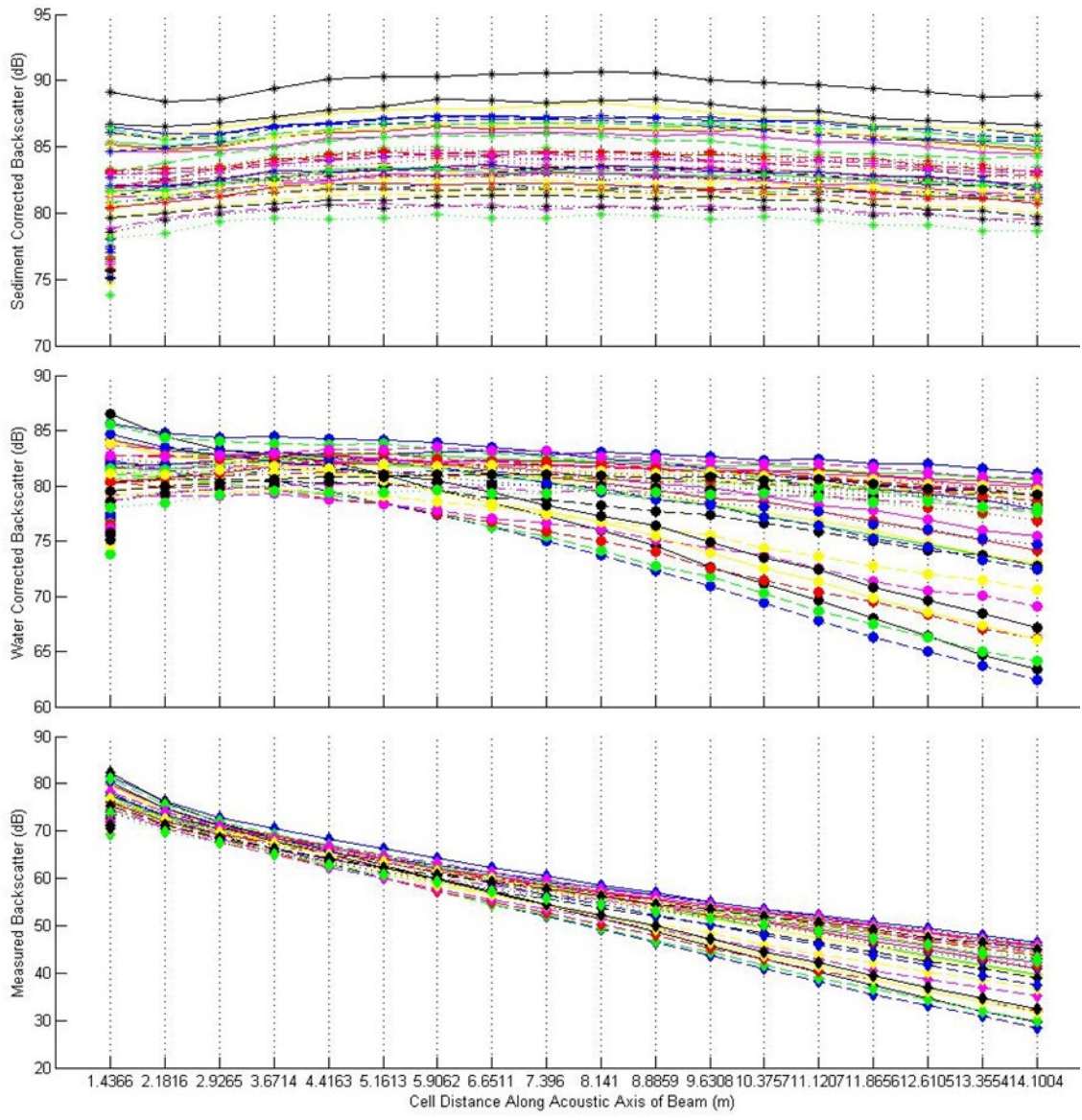


Figure 4-11: Backscatter profile of the Acoustic Doppler Velocity Meter . samples of the 1200kHz side-looking ChannelMaster for the times matching sediment sampling in the Oreti River.

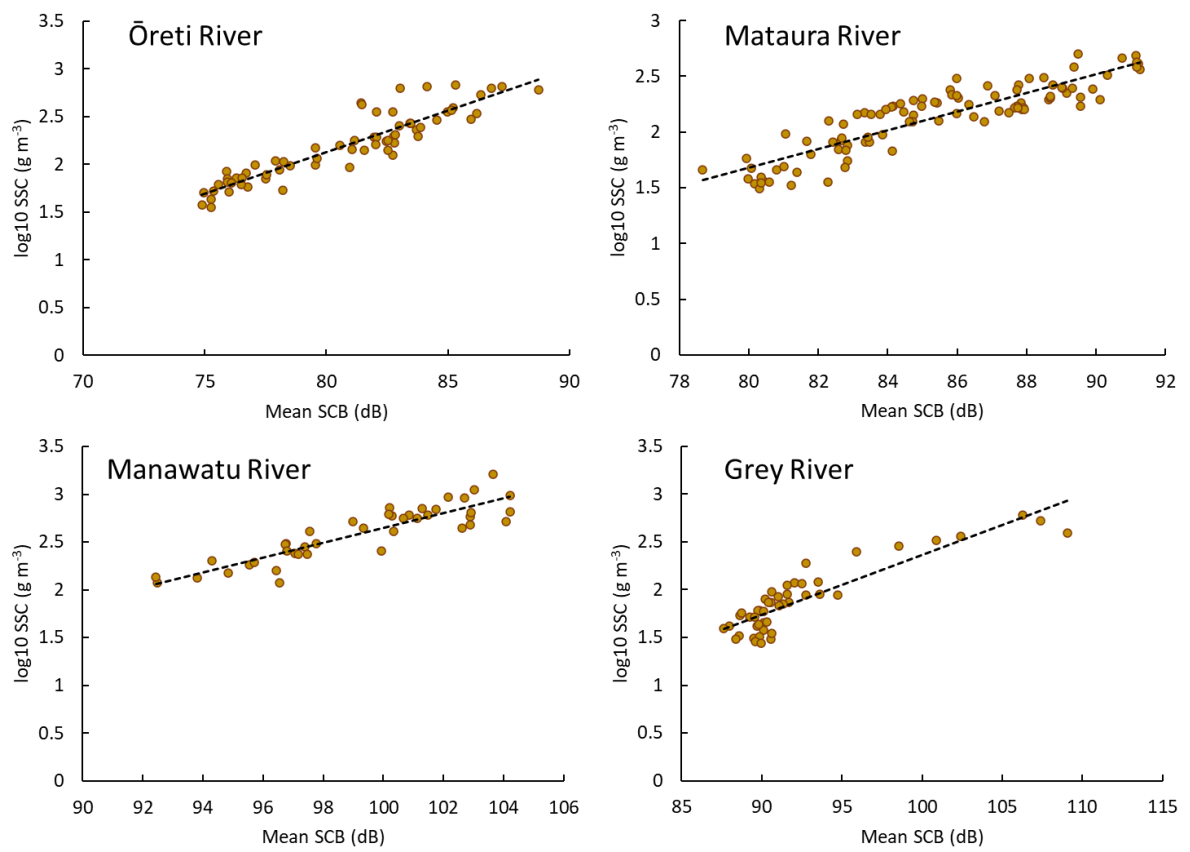


Figure 4-12: Linear regression plot of the log₁₀ SSC against mean sediment corrected backscatter of all four monitored rivers.

Table 4-4: Linear regression model statistics for the SSC measurements using side-looking ADCP sensors at all four monitored rivers.

	Parameters	Estimate	Standard Error	Lower 90%	Upper 90%
Oreti River	Intercept (b_0)	-4.50	0.28	-4.98	-4.03
	Slope (b_1)	0.08	0.00	0.08	0.09
	R-squared	0.91			
	BCF	1.14			
	RMSE (mg l^{-1})	106.3			
Mataura River	Intercept (b_0)	-4.93	0.39	-5.58	-4.28
	Slope (b_1)	0.083	0.0046	0.075	0.090
	R-squared	0.81			
	BCF	1.06			
	RMSE (mg l^{-1})	58.3			
Manawatu River	Intercept (b_0)	-5.15	0.61	-6.18	-4.11
	Slope (b_1)	0.078	0.0061	0.067	0.088
	R-squared	0.81			
	BCF	1.043			
	RMSE (mg l^{-1})	190			
Grey River	Intercept (b_0)	-3.88	0.44	-4.62	-3.12
	Slope (b_1)	0.062	0.005	0.0543	0.0705
	R-squared	0.81			
	BCF	1.068			
	RMSE (mg l^{-1})	79.4			

4.5 Assessing performance of surrogate methods in sediment load estimation

4.5.1 Oreti River

Continuous physical sediment measurements were available for two flood events that occurred in early and late October 2020. These events provided continuous measurements throughout the flood events that could be used to assess measured event loads against event loads estimated from turbidity and side-looking acoustic sensors.

To determine the measured event load for the first flood (6-8 October 2020), 16 automated sediment samples were collected, calibrated to cross-section averaged SSC (see Section 3.2), and then multiplied by concurrent flows to obtain the load (Figure 4-14). Similarly, SSC values derived from turbidity measurements and side-looking ABS measurements were multiplied by their respective flow data to calculate the load. For the second flood event in the Oreti River, 18 sediment samples were used to evaluate the sensors.

It was observed that in both flood events, the measured SSC values showed a closer agreement with SSCs derived from the side-looking ABS sensors (Figure 4-14). This was also reflected in the load estimates, with the side-looking ABS derived event load being only 0.9% higher than the measured event load in Flood number 1 (3635 t compared to 3603 t). The turbidity-derived event load for flood number 1 (2410 t) was 33% less than the measured load. In Flood number 2, side-looking ABS derived event load (9322 t) was 12.5% less than the measured load (10652 t), whereas for the event load (6888 t) derived from turbidity the ratio was 35%.

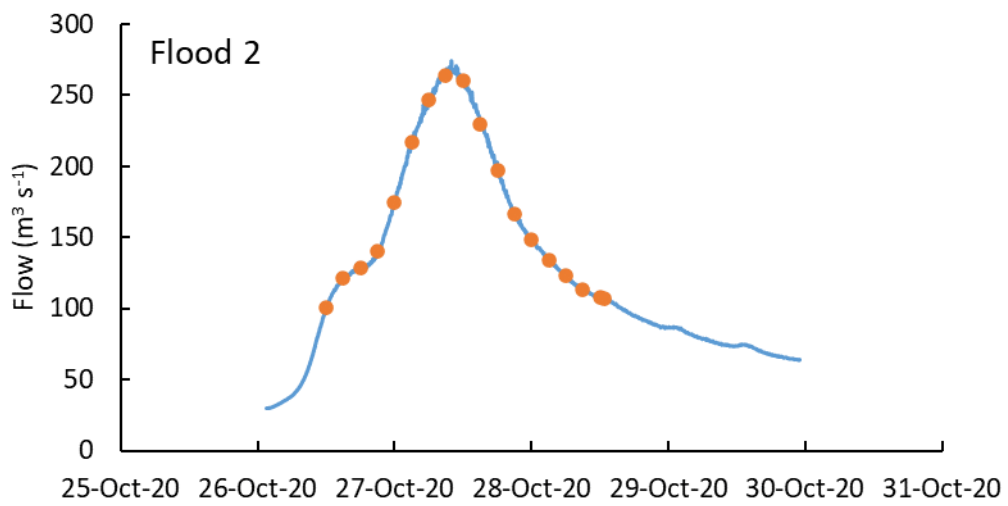
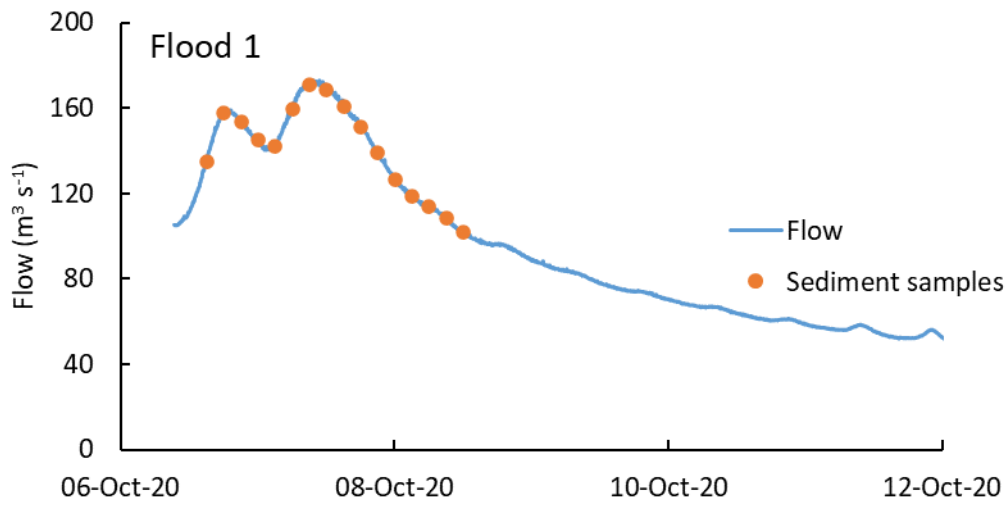


Figure 4-13: Flood events together with collected sediment samples used to evaluate performance of surrogate methods in estimating sediment load at the Oreti River.

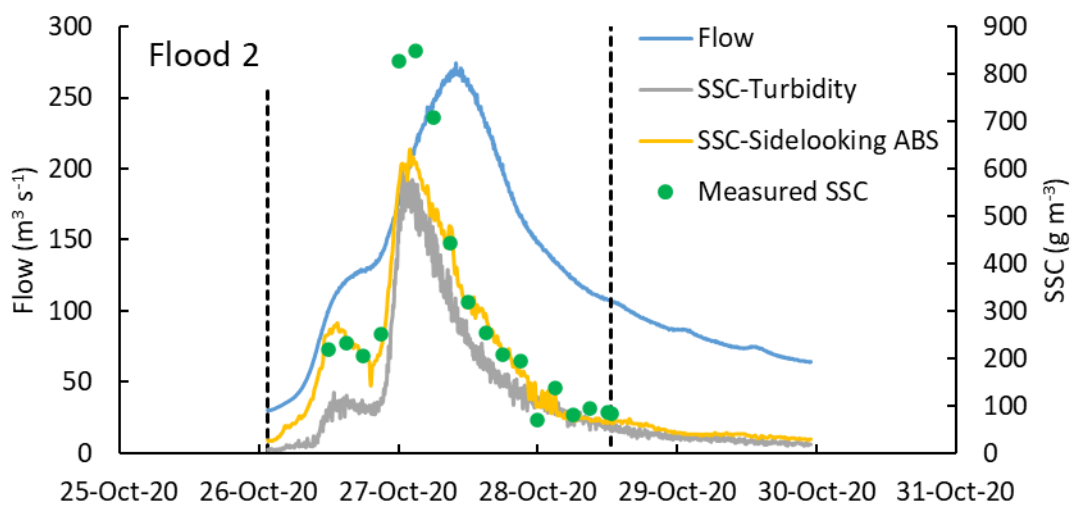
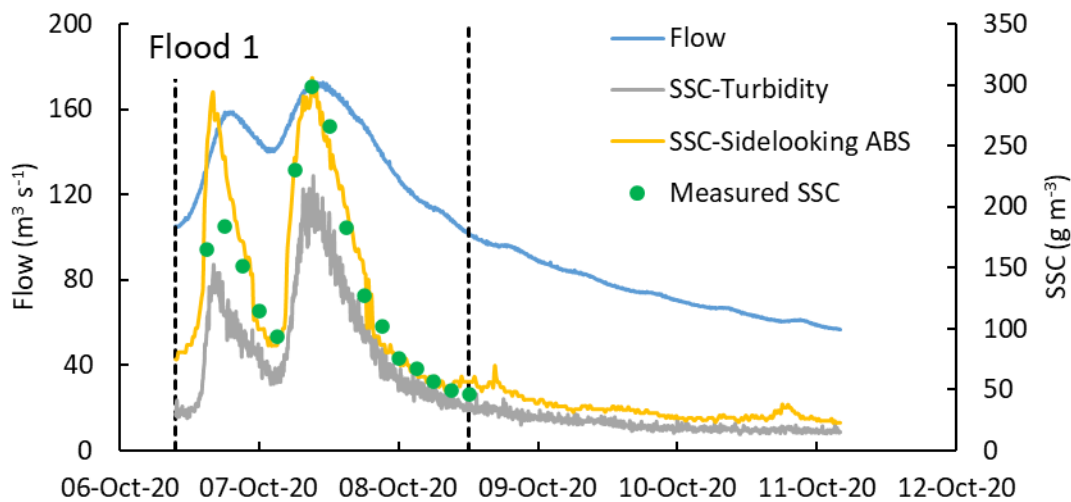


Figure 4-14: Turbidity-derived SSC, ABS side-looking-derived SSC and flow data for selected flood . with complete sediment samples which were used to evaluate sediment load estimates. Dashed vertical lines indicate the time period used to compare sediment loads.

4.5.2 Maitara River

During June 2020, July 2020 and January 2021, a full coverage of sediment measurements across three flood events were used to assess the performance of three sensors (Figure 4-15).

During Floods number 1 and 3, the side-looking ABS sensor demonstrated the least relative error in estimating event load, with a relative error of 3.9% for Flood number 1 and -6% for Flood number 3. In comparison, the turbidity sensor exhibited higher relative errors: -13% for Flood number 1 and 12.6% for Flood number 3, while the at-a-point ABS sensor fared the worst, with relative errors of -35% for Flood number 1 and -52% for Flood number 3 (Figure 4-19, Table 4-5). In Flood number 2, turbidity performed slightly better (relative error of -13.2%) than the side-looking ABS sensor (relative error of 16.5%).

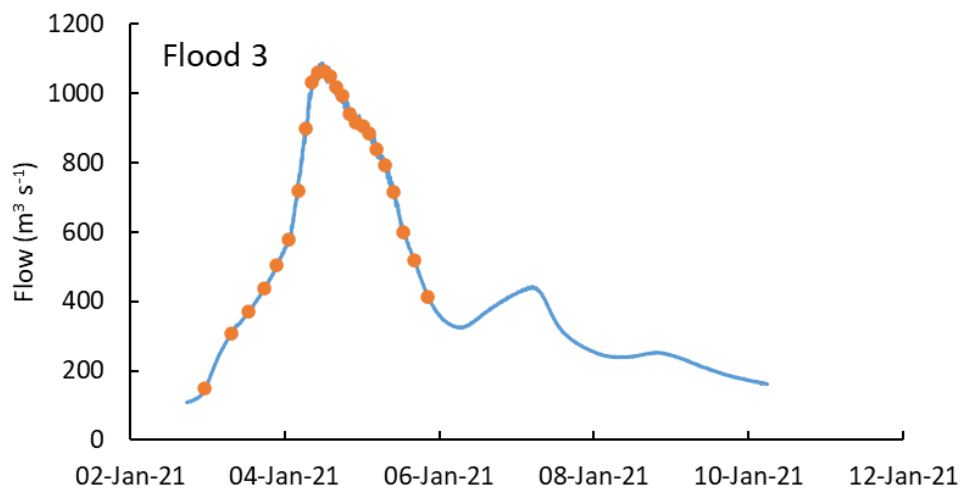
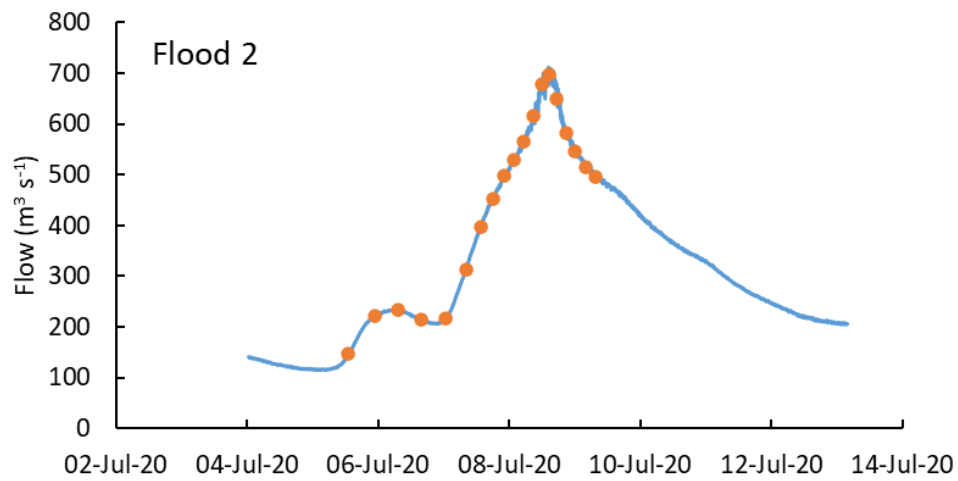
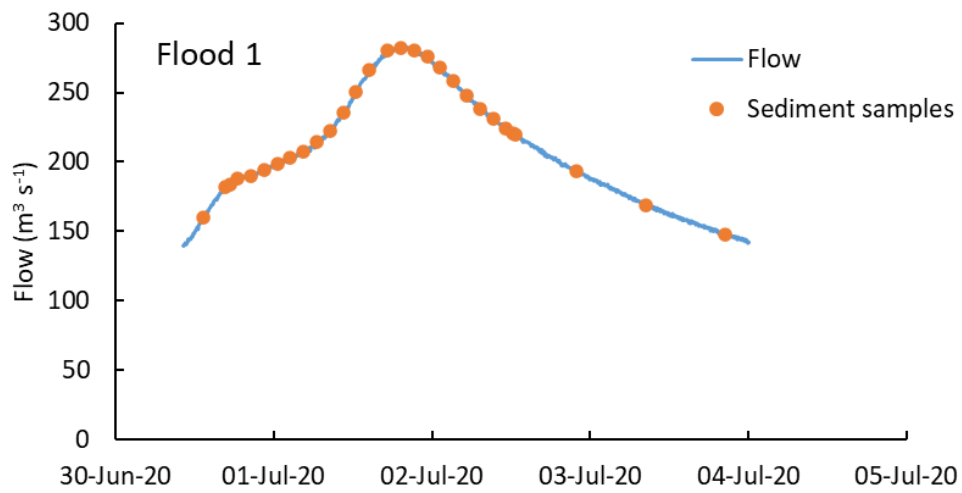


Figure 4-15: Flood events and collected sediment samples used to evaluate performance of surrogate methods in estimating sediment load at the Mataura River.

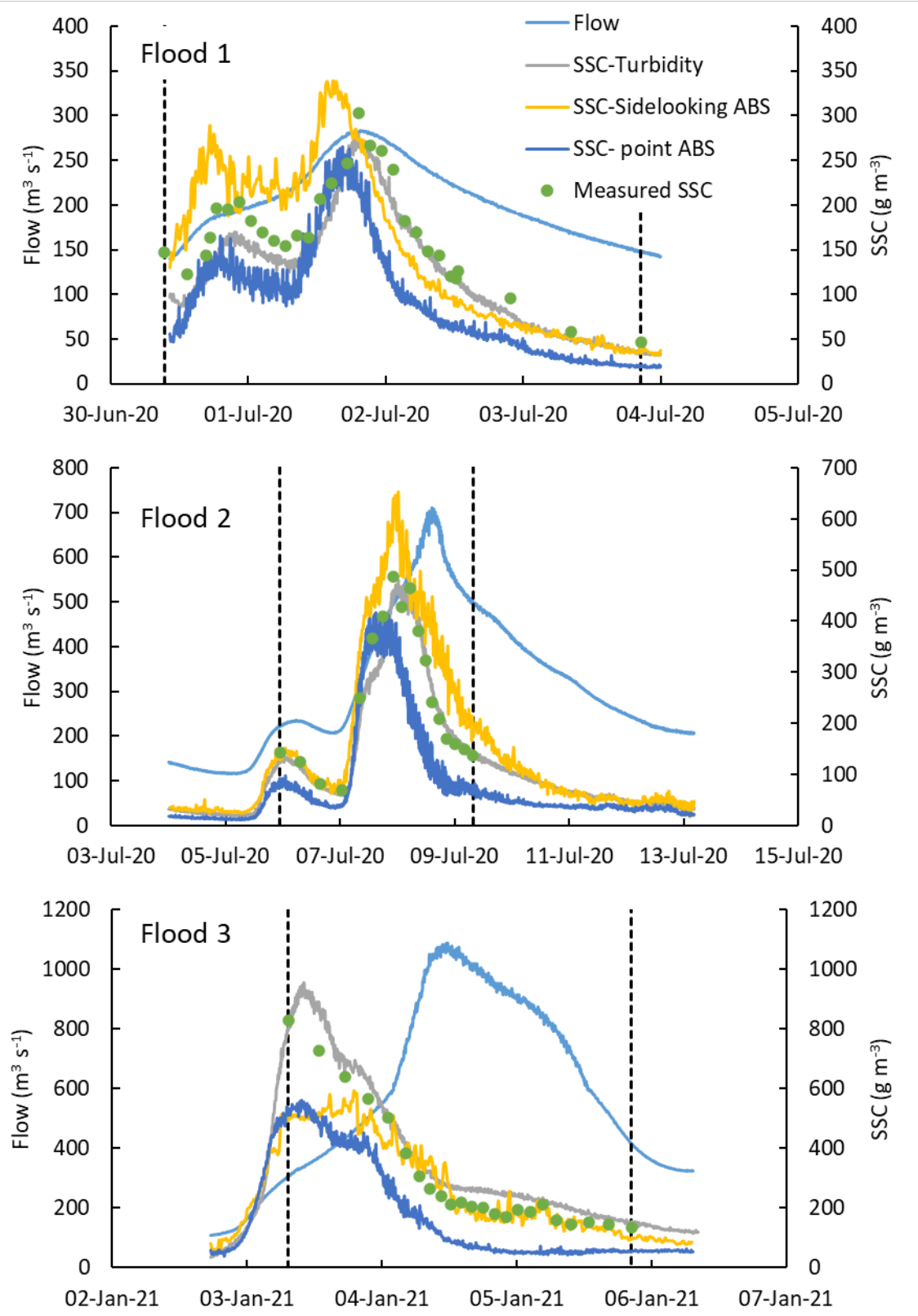


Figure 4-16: Turbidity-derived SSC. ABS side-looking-derived SSC and flow data for selected flood events for which a complete set of sediment samples were used to evaluate sediment load estimates at the Mataura River. Dashed vertical lines indicate the time periods during which sediment loads were compared.

4.5.3 Manawatu River

Manawatu River: During the late November 2022 flood, results from 14 sediment samples were used to compare three surrogate techniques used to measure sediment load (Figure 4-17). When comparing the measured SSC with the surrogate-derived SSC, it became evident that both optical and acoustic at-a-point sensors significantly underestimated the SSC measurements (Figure 4-18). This underestimation was further reflected in the event load estimates, where the loads derived from the at-a-point ABS sensor (1431 t) and turbidity sensor (1820 t) were notably lower than the actual measured load (5106 t). The event load estimate obtained from the side-looking ABS sensor (5935 t) showed only 16% overestimation when compared to the measured load (Table 4-5).

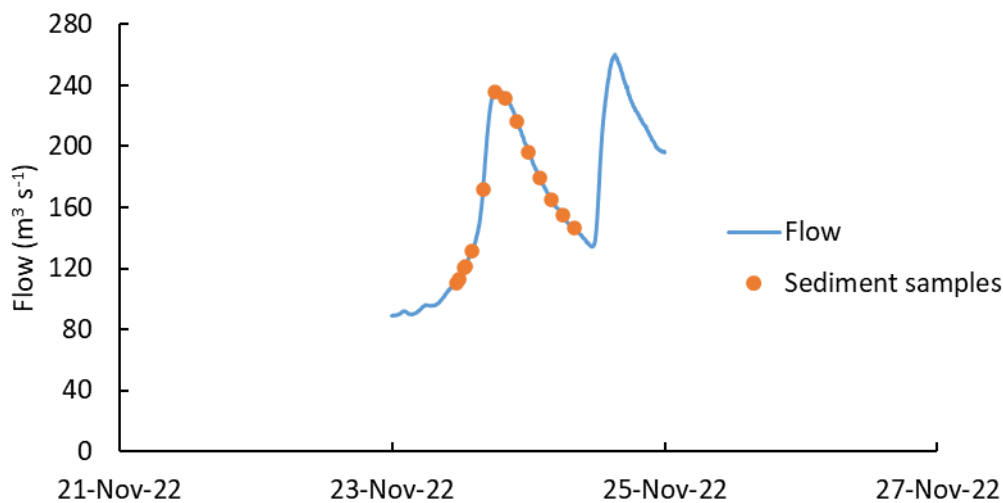


Figure 4-17: Flood event and collected sediment samples used to evaluate performance of surrogate methods in estimating sediment load at the Manawatu River.

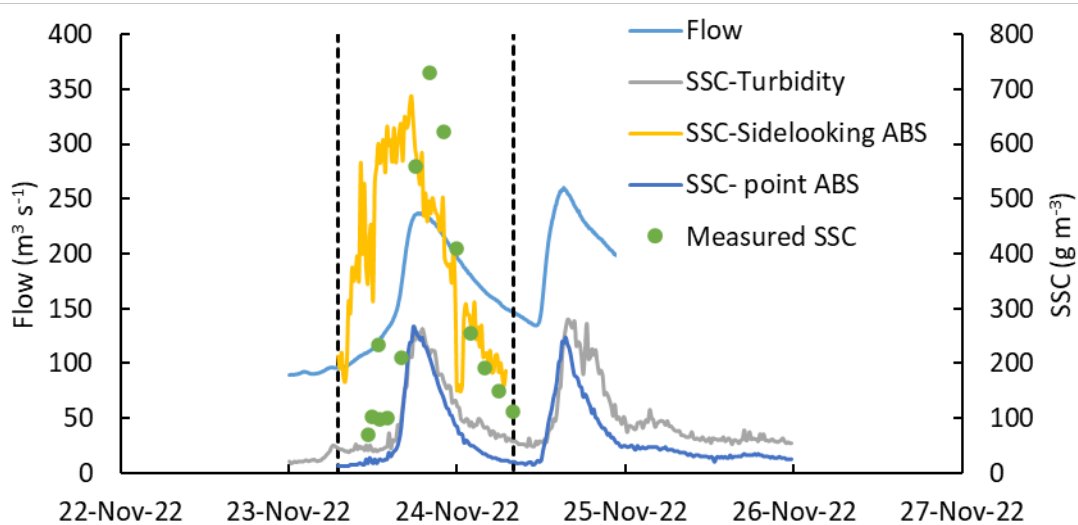


Figure 4-18: Turbidity-derived SSC, at-a-point ABS-derived SSC, ABS side-looking-derived SSC and flow data for selected flood events in the Manawatu River. A sediment sample series was used to estimate sediment load. Dashed vertical lines indicate the time period during which sediment loads were compared.

4.5.4 Grey River

Grey River: Seventeen sediment samples collected during a flood on 31 May 2023 were used to evaluate and compare the performance of the turbidity sensor and the side-looking ABS sensor (Figure 4-19).

When comparing the measured SSC with the SSC values derived from both the turbidity and side-looking ABS sensors, it was evident that the turbidity sensor tends to overestimate sediment concentration measurements (Figure 4-20). This observation was further confirmed when analysing the sediment load estimates. The side-looking ABS sensor-derived event load was found to be only 5% less than the measured load, indicating was able to estimate sediment load during the flood accurately (3736 t compared to the measured load of 3940 t). In contrast, the turbidity-derived event load (5366 t) was 36% larger than the measured load (Table 4-5).

Overall, these findings highlight that the at-a-point ABS and turbidity sensors are not as accurate in estimating sediment load as the side-looking ABS sensor.

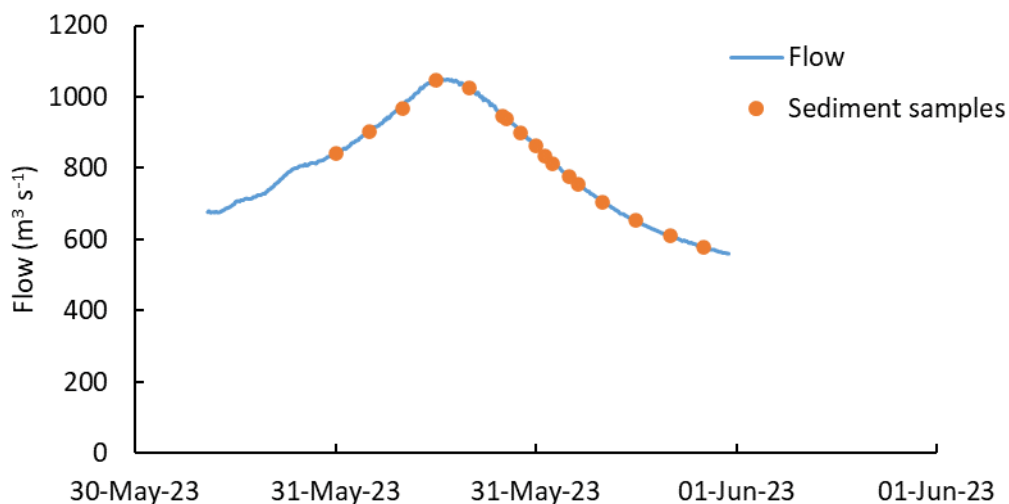


Figure 4-19: Flood event and collected sediment samples used to evaluate performance of surrogate methods in estimating sediment load at the Grey River.

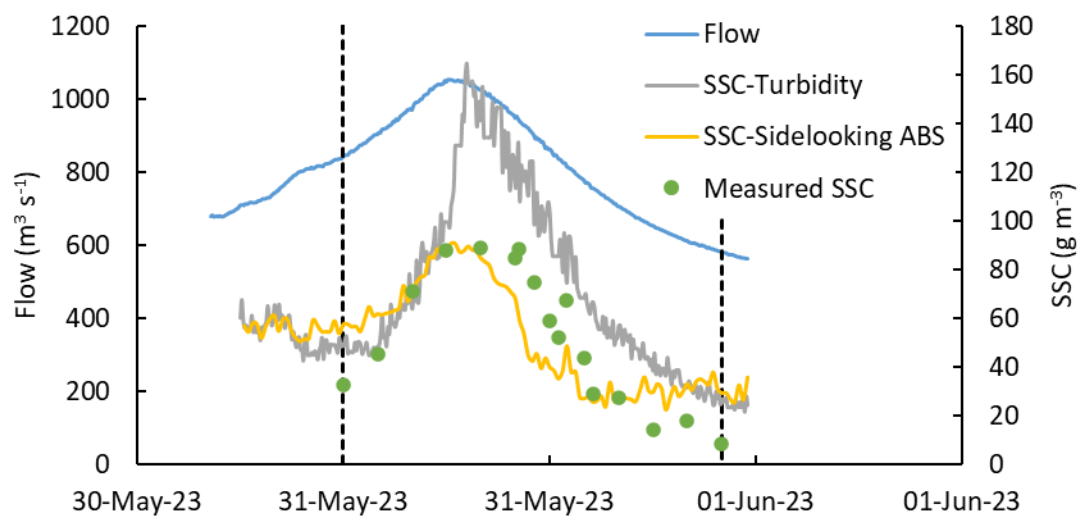


Figure 4-20: Turbidity-derived SSC, ABS side-looking-derived SSC and flow data for selected flood events: with complete sediment samples were used to evaluate sediment load estimates at the Grey River. Dashed vertical lines indicate the time period during which sediment loads were compared.

Table 4-5: Comparing the performance of surrogate techniques in estimating suspended sediment load.

Site	Flood number	Measured event load (t)	Turbidity-derived event load (t)	Relative error for turbidity derived load (%)	ABS-derived event load (t)	Relative error for ABS derived load (%)	ABS side-looking derived event load (t)	Relative error for ABS side-looking derived load (%)
Oreti River	1	3603	2410	-33.1	-	-	3635	0.9
	2	10652	6888	-35.3	-	-	9322	-12.5
Mataura River	1	9607	8328	-13.3	6251	-34.9	9983	3.9
	2	34450	29886	-13.2	20171	-41.4	40127	16.5
	3	46937	52842	12.6	22551	-52.0	44128	-6.0
Manawatu River	1	5106	1820	-64.3	1431	-72.0	5935	16.2
Grey River	1	3940	5366	36.2	-	-	3736	-5.2

5 Summary and recommendations

5.1 The need to calibrate auto-sampled SSC to cross-section averaged SSC

A comparison between the relationships of at-a-point SSC collected by autosamplers and cross-section averaged, depth-integrated SSC obtained through physical sediment samplers (such as depth-integrated or point-integrated samplers) offers valuable insights into the sediment concentration within the river cross section, in contrast to fixed-point sampling conducted from the riverbank. The cross-section averaged SSC did not align with the at-a-point SSC collected by autosamplers at all monitoring sites. This discrepancy arises from uneven mixing of the suspended sediment load throughout the cross section, as well as variations in SSC profile of the different size fraction classes. The process of unmixing and the fluctuation in the ratio of at-a-point SSC to gauged SSC in different rivers is influenced by several factors:

- Turbulence intensity over the cross-section, which changes with water discharge and its cross-sectional distribution,
- The size grading of the suspended sediment load.

In three monitoring sites (i.e., Oreti River, Mataura River, and Manawatu River), the sediment concentration throughout the rivers' cross section was consistently higher than the SSC measured at a single point on riverbanks for all three fractions. For the Grey River, the cross-section averaged SSC was lower than the auto-sampled SSC. Although it is less common for the gauged cross-section averaged SSC to be lower than the auto-sampled SSC, there is nothing abnormal or concerning about this result. It simply indicates that the SSC at the sampler intake point was higher than the spatial average SSC across the cross section.

5.2 Sediment concentration measurements using turbidity sensors

The key findings derived from the comparison of turbidity data in various rivers are as follows:

- There is no standard conversion between turbidity values and quantitative mass measurements of the sediment as SSC.
- Various turbidity sensors exhibit distinct numerical responses, even when measuring sediment concentrations with similar characteristics (from a same monitoring site). This has been observed by comparing four different ISO 7027 compliant turbidity sensors (Hach-Solitax, Observator, ExoSonde, and DTS-12 sensors) in the Mataura River during a similar flood event³. Turbidity readings from the flood event in November 2019 reveal a significant variation in turbidity response (about 2-fold) in different sensors (Figure 5-1). The variation in numerical response among turbidity sensors has been acknowledged in previous studies (Rymaszewicz et al. 2017; Davies-Colley et al. 2021a).
- Not only do different turbidity sensors exhibit distinct responses, but even similar turbidity sensors can yield different correlation results in different rivers. For instance, when comparing the correlation coefficients between turbidity and total SSC obtained from the Observator sensor deployed in the Grey River (regression coefficient = 2.57)

³ The comparison of various turbidity sensors was not within the scope of the Envirolink project's objectives. This comparison was conducted independently as part of the NIWA Strategic Science Investment Fund (SSIF) - high frequency water quality monitoring research project.

to those from the same sensors, with identical calibration to formazin, used in the Oreti River (regression coefficient = 0.65), a significant disparity is observed. Notably both sensors followed linear regression with zero intercept. This discrepancy in correlation results highlights the sensitivity of turbidity measurements to the specific sediment characteristics and organic materials present in different river systems.

- Nevertheless, it is essential to note that the outputs of the two turbidity sensors used in these case studies exhibit a robust linear correlation with sediment concentration. This strong correlation implies that if turbidity values are locally calibrated to mass measurements of sediment, it becomes possible to compare standardised sediment concentrations derived from sites with different sediment characteristics or using different turbidity sensors.
- None of the turbidity sensors should necessarily be deemed superior to the others, unless a sensor or sensor-type demonstrates a non-linear response, excessive drift, or unstable response to a standard. Turbidity measurements are qualitative rather than quantitative in nature.
- Turbidity sensors saturate at moderately high SSCs during flood peaks even when calibrated with high range Formazin standards. This can significantly impact suspended sediment load estimates, since suspended sediment load are at the maximum during this period. **Error! Reference source not found.** shows an example of turbidity range limitation in Rangitata River at Gorge using an Observer turbidity sensor calibrated to its highest reading range.

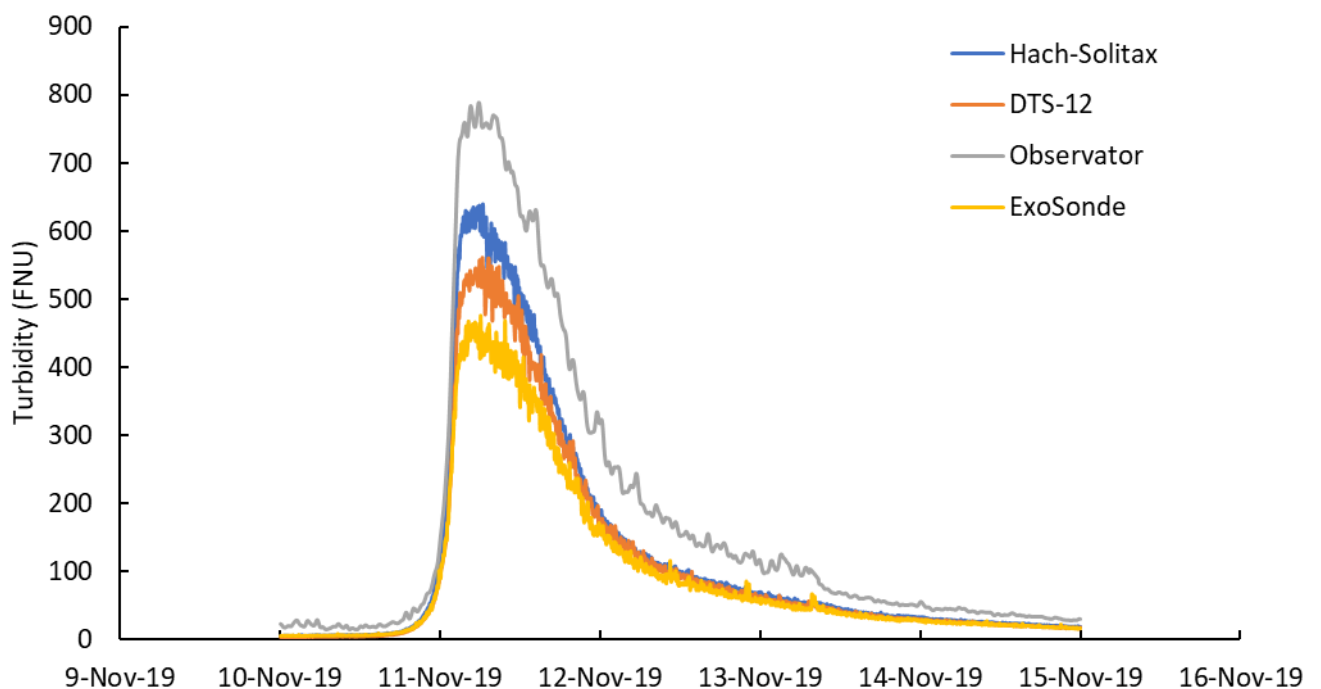


Figure 5-1: Turbidity measurements from four different sensors during November 2019 event at the Mataura River. The sensors used for this comparison were all calibrated to the Formazin standard in the NIWA laboratory.

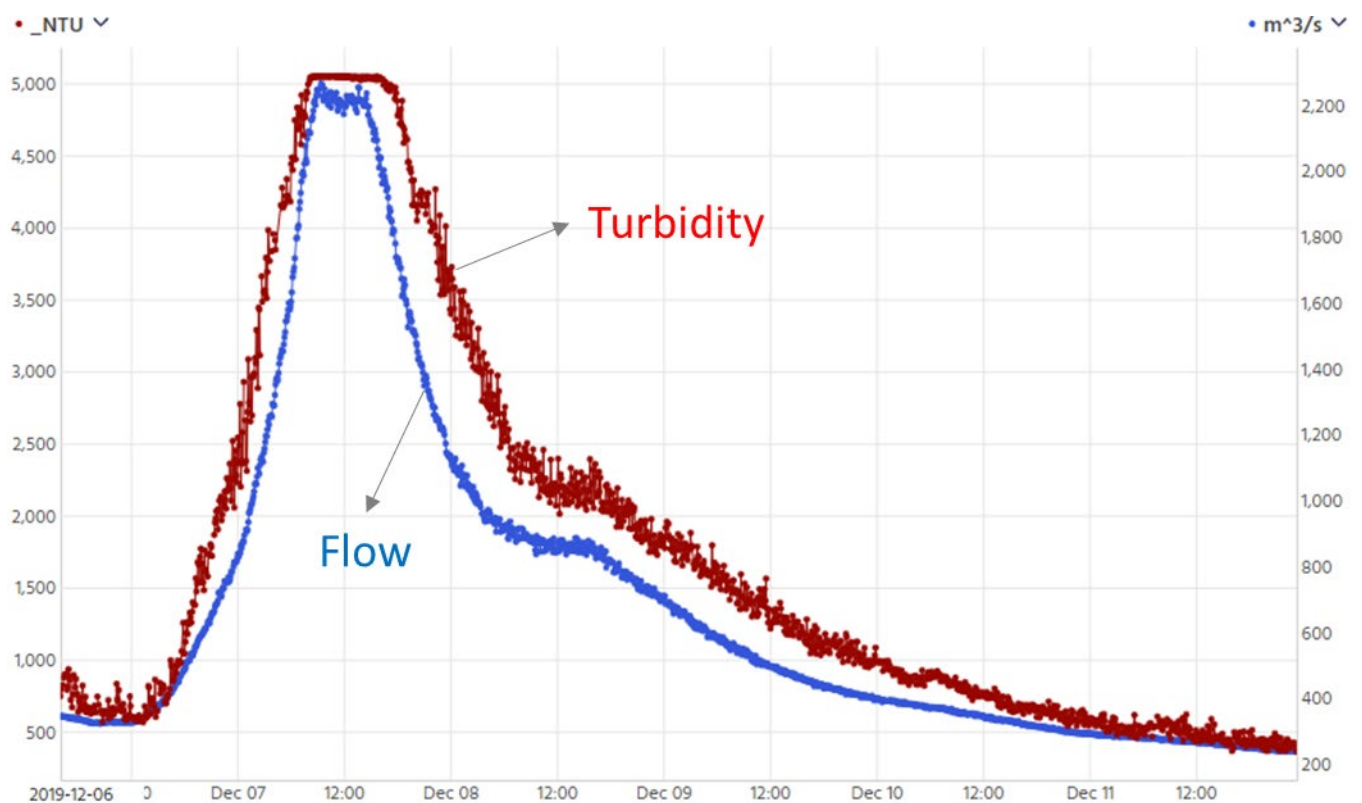


Figure 5-2: Saturation of turbidity sensor during high flows in Rangitata River at Gorge site. Note that Rangitata River is not one of the monitoring sites used in this study, but the sensor used here is similar to the one in the Oreti and Grey Rivers.

5.3 Sediment concentration measurements using at-a-point acoustic backscatter sensors

Upon comparing the results of the at-a-point optical and ABS sensors at two monitoring sites, it becomes evident that the ABS sensor establishes a notably superior relationship with sediments possessing coarser than 63 μm fractions (i.e., sand SSC) in comparison to the turbidity sensor. Conversely, the turbidity sensors demonstrate a stronger relationship to silt and finer suspended sediments. Therefore, since at-a-point ABS sensors are more responsive to sand and less to fine silt and clay, they provide more accurate estimates of sediment load in situations where coarser sediments predominate.

Comparing sediment load estimates derived from at-a-point ABS and turbidity sensors reveals that ABS sensors significantly underestimate event load at these monitoring sites compared to turbidity-derived load. This discrepancy occurs because the sediment concentration of silt and finer fractions during the measured events in the monitoring sites is notably higher than that of the sand fraction. Additionally, ABS sensors become less responsive as the grainsize decreases below 32 microns (i.e., medium silt and finer), leading to their total load estimate being lower than the measured load when compared to turbidity sensors.

At-a-point ABS sensors have a reasonably flat and strong response to sand sediments, making them valuable in situations where the objective of the monitoring is to estimate sand load accurately, as was the case in a study by Haddadchi et al. (2022) in the lower Waiau River, Southland New Zealand.

The river has quite variable size grading during different phases of the flood, resulting from the variability in sediment sources' lithology in the upstream catchment.

- In such situations, using both optical and acoustic sensors can offer valuable insights into the dynamics of sediment transport, considering the size grading throughout different phases of flood events and their environmental impacts (e.g., deposition of coarser sediment during the recession of flood events).
- An example of data measured during a flood in December 2019 in the Mataura River in Figure 5-3. is illustrative:
 - more sand (indicated by ABS records) was transported during the rising limb of the second flow peak,
 - silt and finer materials (indicated by turbidity records) were transported at high concentration at the start of the flood and during the flow peak.

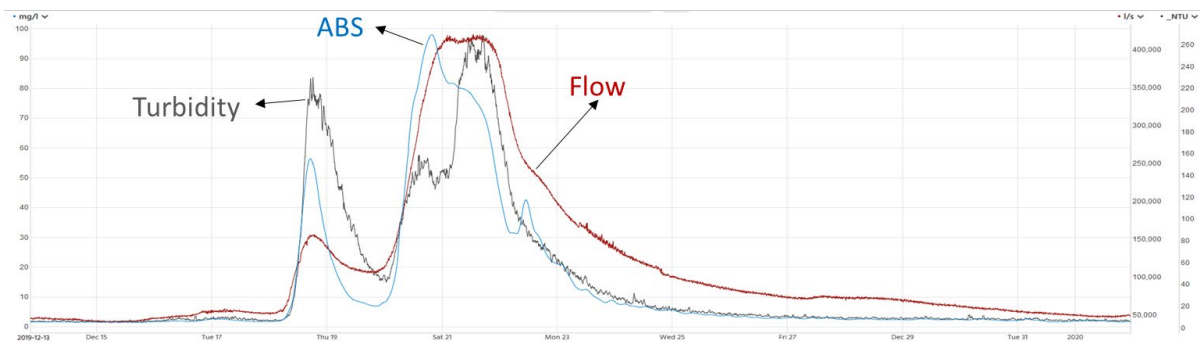


Figure 5-3: Data acquired during a flood in Mataura River showing patterns of sediment movement during the event. measured by optical turbidity and acoustic LISST-ABS sensors.

5.4 Assessing performance of surrogate methods in sediment load estimation

In flood events with complete sediment sampling coverage throughout the event, ABS side-looking sensors demonstrated higher accuracy in estimating sediment load compared to at-a-point optical and acoustic sensors at all monitoring sites (Table 4-5). This is because side-looking sensors capture variability of the sediment concentration across the entire cross-section (or the 'sonified' section of the river) as opposed to the SSC index measured by at-a-point sensors located next to the riverbank. For example, during flood number 1 in the Oreti River, the ABS side-looking sensor recorded a SSC of 254 g m^{-3} at the peak of flood (7/10/2020 9:15) at the true left bank. As measurement point moved 7.3 m from the left bank, the SSC increased to 341 g m^{-3} . In contrast, at the same time step, the SSC estimated using turbidity data was 226 g m^{-3} , measured only at the riverbank. Similarly, during flood number 2 in the Oreti River, the ABS side-looking SSC near the riverbank was 532 g m^{-3} , which increased to 800 g m^{-3} in the middle section of the river channel. In comparison, the turbidity-derived SSC measured at the riverbank was 571 g m^{-3} (Figure 5-4).

These findings clearly indicate that the at-a-point sensors are unable to accurately represent changes in sediment concentration throughout the cross-section, even when calibrated using cross-section averaged, discharge-weighted SSC. The cross-section averaged, discharge-weighted SSC data were only collected a few times during the flood events and were insufficient to capture the dynamic

changes in SSC across the river cross-section at high temporal resolution. Side-looking sensors enable “continuous” measurement of SSC across the river cross-section at a high frequency (here, every 15 minutes), which permits high temporal resolution of sediment dynamics. This higher sampling frequency enables better understanding of the sediment concentration during a flood.

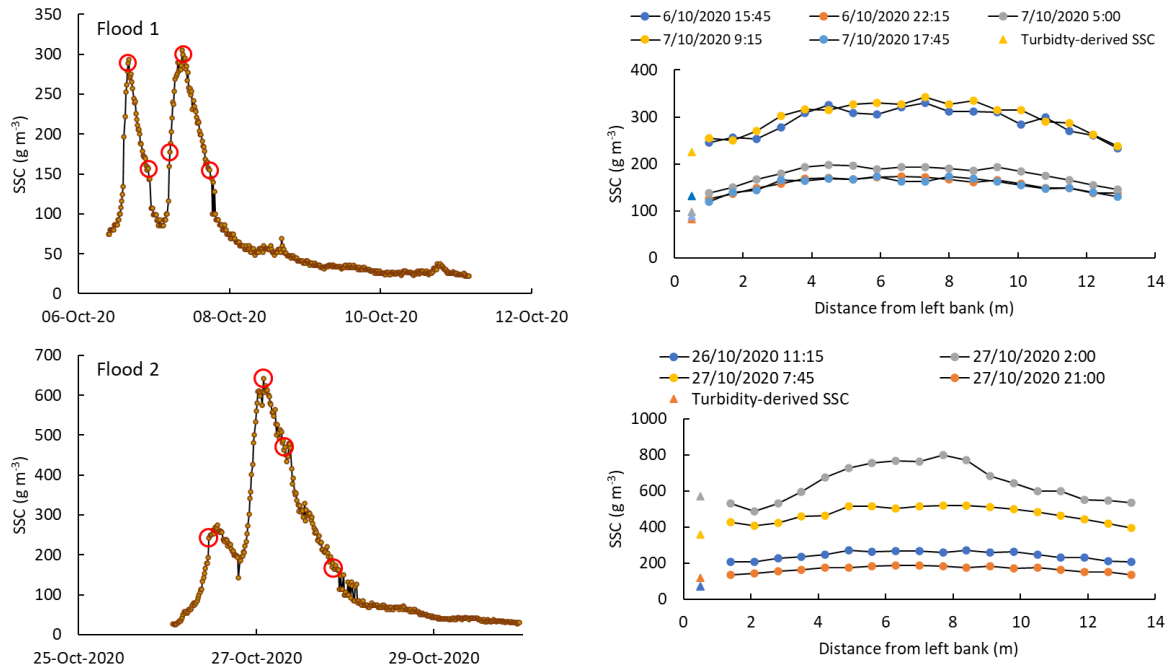


Figure 5-4: Average SSC (left plots) and its cross-sectional variation (right plots) in two example floods at the Oreti River. The times when cross sectional variation of SSC was measured (right plot) are indicated by red circles in left plot.

Data derived from side-looking sensors allows development of sedigraphs for each bin within the river cross-section (or for each section of the river by averaging bin values). Example sedigraphs are shown in Figure 5-5 for different bins throughout the cross section during two Oreti flood events. This can offer valuable insights into horizontal sediment mixing within the rivers during the flood events. For example, the greatest SSC occurs in a bin centred at 7.1 m etc., and reliance on SSC measurements derived from samples collected in the 1 m bin will underestimate SSC (and therefore sediment load) quite significantly.

This feature is especially beneficial in situations where a tributary with a high sediment concentration joins the main channel upstream of the monitoring site. By using side-looking sensors, we can isolate and assess the sediment load estimate for each section of the river, which helps in understanding the spatial variation and the dynamics of sediment transport within the river cross-section and quantify the amount of sediment load coming from the tributary. Similarly, in braided river systems where shear velocity significantly varies within the cross section, side-looking sensors allow us to analyze sediment patterns and load estimates accurately for different sections of the river.

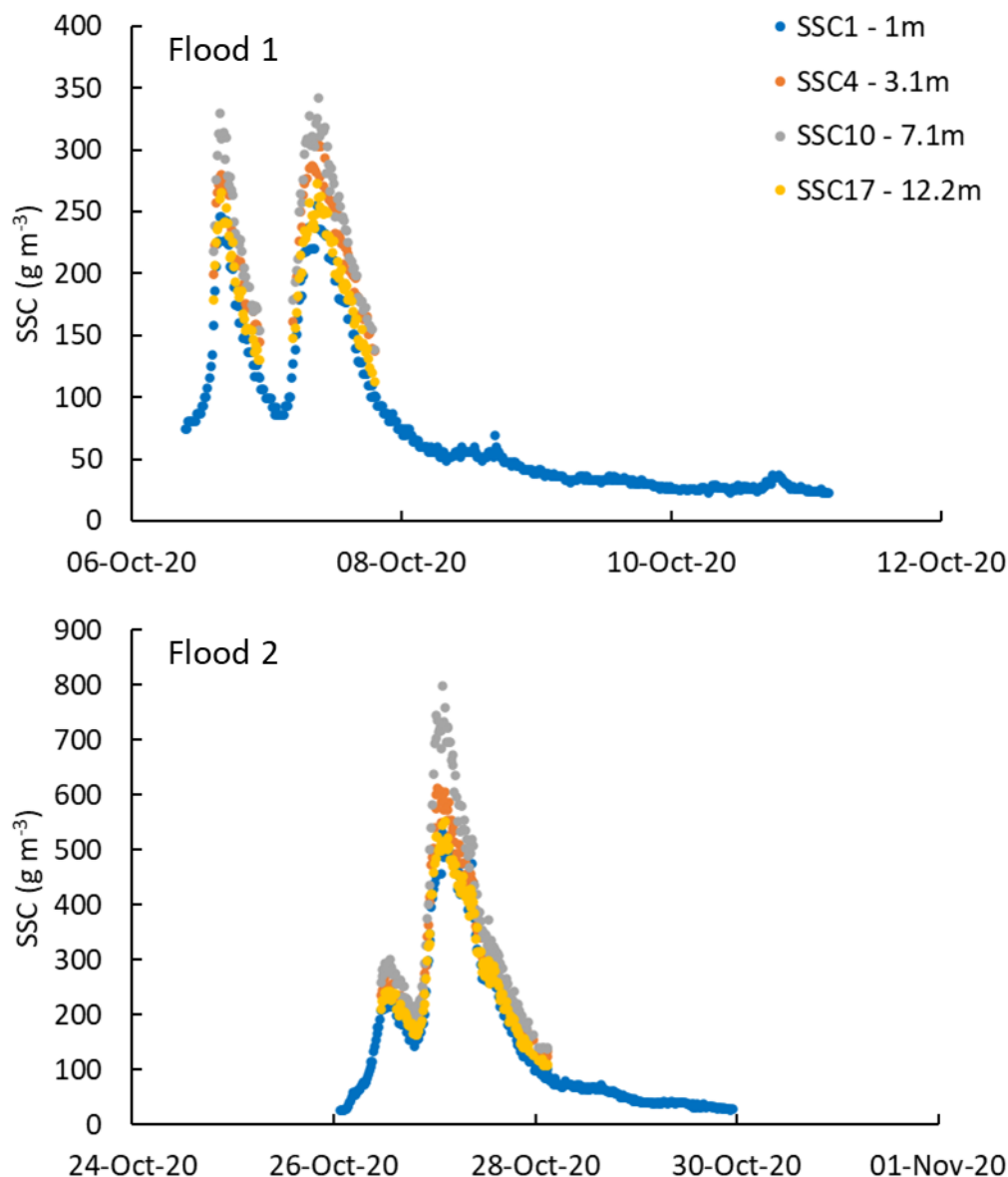


Figure 5-5: Variation of SSC at four bins during the two example floods at the Oreti River. The four bins indicate variation in SSC across the river cross-section, measured from the true left bank.

5.5 Field experience with use of surrogate technologies

5.5.1 Installation and Operation of Acoustic Side-lookers

The ADCP sensors were installed on the banks of the rivers using rail mount systems. These sliding rail systems made the sensors easily accessible for service and cleaning (Figure 5-6) and ensured that the sensors could be returned to the same fixed position after servicing. The sliding rail mount did require some extra care during the setup time to set the instrument pitch and roll as close as possible to level so the acoustic path was horizontal across the river.

Setting up the site, installing the sliding rail mount, and levelling the side-looking sensors can be labour-intensive and may become expensive for projects and monitoring operations with limited

financial resources. This is the primary installation drawback of the side-looking sensors when compared to at-a-point sensors.

At the Maitara River, the side-looking ADCP sensor was first installed in May 2016 on the true left bank approximately 40 m downstream of the main bridge site where the level, turbidity, water quality and autosampler instruments were situated. This location was chosen to have a clear acoustic path across a relatively deep section of the channel. We anticipated some disturbance from wake turbulence generated by the bridge piers, but this could not be avoided at the time of the installation due to a limit on the maximum available cable length back to the recorder housing infrastructure at the bridge. Examination of the initial record showed that wake turbulence from the bridge piers had a significant impact on the acoustic signal across the river which meant analysis for acoustic sediment derivation would not be possible. So, in February 2019 the instrument and rail system were moved to a new location 150 m downstream of the bridge where flow was relatively laminar across the channel. Therefore, when installing the ADCP sensor it is important to choose a location far from bridges or hydraulic structures to avoid the impact of turbulence in flow caused by these structures.

For the Oreti, Mataura and Grey River sites, data were collected internally utilising the 4MB internal recorder which could hold 40 days of record. The full cross section ABS intensity and velocity raw data is a binary Teledyne format data file that can be exported to CSV files. Cleaning the instrument, checking and downloading the internal recorder took at least 1 hour on site per month. For Manawatu River, the ADCP sensor was telemetered and acoustic data from all bins were transferred instantaneously to the server.

We found that the ADCP instruments required very little maintenance other than a clean of the sensor faces when we could access them.

At the Maitara site, cleaning the faces of the sensor did become more difficult after the very large flood in February 2020, which caused a some bank on the left bank upstream of the installation. Debris generated by upstream bank erosion may cause the sliding rail carriage to jam. Therefore, it is important to install the sensor where the bank is protected from erosion as far as possible.

During very large flood events, when a large amount of debris and slash may pass the sensor, the acoustic data reading may be disrupted. For example, during the very large ($2300 \text{ m}^3 \text{ s}^{-1}$) flood at the Maitara River on 5 February 2020, data collection continued, but data quality was affected by the large amounts of debris coming past and striking the sensors. The pitch and roll data showed considerable noise over this period and this appears to have caused noise in the intensity and velocity records.



Figure 5-6: A sliding rail mount at Matura River and cleaning the sensor by Andrew Willsman (NIWA-Dunedin).

5.5.2 Operational summary – side-looking ADCP vs at-a-point sensors

Using side-looking instruments to measure acoustic signal as a suspended sediment surrogate is more costly and somewhat more complicated than operating at-a-point sensors (e.g., Sequoia LISST ABS or turbidity sensors). The differences and benefits of these two different technologies are summarised in Table 5-1.

Table 5-1: Comparing side-looking and at-a-point optical and acoustic sensors.

Consideration	Side-looking ADCP	At-a-point sensors	Difference
Cost	Instruments are approximately 20,000 USD.	Instrument prices range significantly. At-a-point ABS are approximately 5,000 USD.	Significant.
Location – cross section	Require a laminar cross section with a sufficiently large depth to width ratio to enable horizontal profiling without the bed interfering with the beam.	Only require enough depth at the sensor so optical or acoustic interference does not occur.	Side-looker will profile the full width of channel and may pick cross channel changes.

Consideration	Side-looking ADCP	At-a-point sensors	Difference
Installation hardware	Require a rigid mounting system that holds pitch and roll near zero. Usually needs to be a more expensive rail system to allow the instrument to be removed for cleaning.	Require a relatively simple robust bank mount only.	Cost (side-looker may require a rail system costing at least \$5000) and some extra installation complexity.
Maintenance - ongoing	Acoustic sensors are robust. Electronics are very stable with no issues with any instruments. We operated these devices in situ with an approximate monthly cleaning cycle. Performance does not appear adversely affected by biofouling if devices are cleaned less frequently.	Acoustic sensors are robust instruments. Biofouling cleaning can be done monthly (or even less frequently if required). Optical sensors do require thorough monthly cleaning, as well as wiper systems, which also require maintenance.	Both Acoustic sensor types could be left for periods longer than 1 month without cleaning with no apparent issues. Optical sensors require wipers, and intermittent cleaning (monthly or bi-weekly dependent on the sensor coating). Wiper maintenance increases overall maintenance requirements.
Power requirements	If telemetry is not required, these instruments can be run with modest solar power supplies. The addition of microprocessors and wireless routers for telemetry uses relatively large amounts of power.	Low power devices.	Power requirements for telemetry, independent of the measurement device.
Data management	Large amounts of data need to be collected to retrieve the acoustic signal intensity. During out trial only large raw binary data files were collected and retrieved. The manufacturers are implementing new firmware to allow SDI12 retrieval of acoustic signal data (in addition to the already available velocity data).	Small data volumes which can be easily retrieved through digital signal (SDI12) to standard datalogger telemetry.	Data quantity, type, and derived information capability.

Consideration	Side-looking ADCP	At-a-point sensors	Difference
Data storage	Downloaded raw binary files were processed to retrieve the acoustic signal profile time series, which can then be imported into database management software.	Single data point time series in a database.	Large amount of data vs small amount, data manipulation requirements.
Supplementary information – velocity and flow	Velocity profiling (bidirectional) and stage measuring (pressure and uplooking acoustic) is standard. One instrument can be a full index velocity flow station that can measure flow where standard stage discharge ratings will not work. Velocity and stage data outputs to telemetry easily.	No additional sensors.	Side-lookers can also derive flow at locations where standard stage discharge stations will not work e.g., tidally influenced locations.
Additional information – suspended sediment	Cross channel variation may potentially be picked up, and with the possibility of using two frequencies different sediment sizes may be detected.	No additional parameters.	More information from a side-looker.
Post-processing of raw data	No data cleaning is required. However, the collected acoustic data from each bin need to be combined and analysed to change backscatter to water-corrected backscatter and sediment-corrected backscatter	Point acoustic and turbidity data need cleaning to remove spikes	More data processing is required for side-looking ADCP.
Deriving SSC for continuous surrogate records after making calibration	Need extensive data processing to convert acoustic measurement to sediment-corrected acoustic data.	After cleaning the data, simple regression coefficients may be applied to acoustic or turbidity measurements to derive SSC.	More data processing is required for side-looking ADCP.

6 Acknowledgements

We would like to thank Horizons regional Council staff (Michaela Rose, Paul Peters, Andrew Swanny) for their help in providing surrogate data and also doing sediment gauging during flood events at the Manawatu Teachers College site. We would like to thank NIWA technicians who helped during sediment gauging campaign: Michael O’Driscoll, John Porteous, Darren Gerretzen (NIWA-Greymouth) for works on the Grey River; Adrian Aarsen, Elliot Bowie, Eric Stevens (NIWA-Dunedin) for works on the Maitai and Oreti Rivers. We would like to specifically thank Brent Watson (Council champion for this Envirolink Tools project) who provided a great deal of support and advice during this project.

7 Glossary of abbreviations and terms

H-ADCP	Horizontal Acoustic Doppler Current Profiler
ABS	Acoustic Backscatter
SSC	Suspended sediment concentration
NEMS	National Environment Monitoring Standard
NPS-FM	National Policy Statement for Freshwater Management
ISO7027	An ISO standard for water quality that enables the determination of turbidity.

8 References

- Davies-Colley, R., Hughes, A.O., Vincent, A.G., Heubeck, S. (2021a) Weak numerical comparability of ISO-7027-compliant nephelometers. Ramifications for turbidity measurement applications. *Hydrological Processes*, 35(12): e14399. <https://doi.org/10.1002/hyp.14399>
- Davies-Colley, R.J., Heubeck, S., Ovenden, R., Vincent, A., Payne, G., Hughes, A. (2021b) Numerical comparability of ISO 7027-compliant nephelometric turbidity sensors commonly used in New Zealand. *Prepared for Envirolink*.
- Domanski, M.M., Straub, T.D., Landers, M.N. (2015) Surrogate Analysis and Index Developer (SAID) tool (version 1.0, September 2015). *U.S. Geological Survey Open-File Report 2015–1177*: 38. <http://dx.doi.org/10.3133/20151177>
- Haddadchi, A., Hicks, M. (2020) Understanding the effect of catchment characteristics on suspended sediment dynamics during flood events. *Hydrological Processes*, 34(7): 1558-1574. [10.1002/hyp.13682](https://doi.org/10.1002/hyp.13682)
- Haddadchi, A., Hicks, M., Hoyle, J., Willsman, A. (2022) The sand load of the Lower Waiau River at Tuatapere. Prepared for Meridian Energy Limited. . *NIWA Client Report: 2022023CH*.
- Landers, M., Arrigo, J., Gray, J.R. (2012) Advancing hydroacoustic technologies for sedimentology research and monitoring. *Eos, Transactions American Geophysical Union*, 93(26): 244-244. [10.1029/2012eo260007](https://doi.org/10.1029/2012eo260007)
- Landers, M.N., Straub, T.D., Wood, M.S., Domanski, M.M. (2016) Sediment acoustic index method for computing continuous suspended-sediment concentrations. *U.S. Geological Survey Techniques and Methods, book 3, chap. C5*: 63. <http://dx.doi.org/10.3133/tm3C5>
- Medalie, L., Chalmers, A.T., Kiah, R.G., Copans, B. (2014) Use of acoustic backscatter to estimate continuous suspended sediment and phosphorus concentrations in the Barton River, northern Vermont, 2010-2013. *Open-File Report*: 41. [10.3133/ofr20141184](https://doi.org/10.3133/ofr20141184)
- Ministry for the Environment and Ministry for Primary Industries (2018) Essential Freshwater: Healthy Water, Fairly Allocated.
- NEMS-Water Quality (2019) National Environmental Monitoring Standards -Turbidity v1.2. <https://www.nems.org.nz/documents/turbidity-recording/>
- NPS-FM (2020) National Policy Statement for Freshwater Management 2020, New Zealand Government August 2020. <https://environment.govt.nz/publications/national-policy-statement-for-freshwater-management-2020/>
- NZCPS (2010) New Zealand Coastal Policy Statement.
- Rymaszewicz, A., O'Sullivan, J.J., Bruen, M., Turner, J.N., Lawler, D.M., Conroy, E., Kelly-Quinn, M. (2017) Measurement differences between turbidity instruments, and their implications for suspended sediment concentration and load calculations: A sensor inter-comparison study. *Journal of Environmental Management*, 199: 99-108. [10.1016/j.jenvman.2017.05.017](https://doi.org/10.1016/j.jenvman.2017.05.017)

- Topping, D., Wright, S., Melis, T., Rubin, D. (2007) High-resolution measurements of suspended-sediment concentration and grain size in the Colorado River in Grand Canyon using a multi-frequency acoustic system. *Proceedings of the 10th international symposium on river sedimentation*.
- Topping, D.J., Wright, S.A. (2016) Long-term continuous acoustical suspended-sediment measurements in rivers—Theory, application, bias, and error. *U.S. Geological Survey Professional Paper: 98*. <http://dx.doi.org/10.3133/pp1823>
- Topping, D.J., Wright, S.A., Griffiths, R., Dean, D. (2015) Physically based method for measuring suspended-sediment concentration and grain size using multi-frequency arrays of acoustic-doppler profilers. *Proceedings of the Third Joint Federal Interagency Sedimentation Conference on Sedimentation and Hydrologic Modeling, Reno, Nevada*.
- Wall, G.R., Nystrom, E.A., Litten, S. (2006) Use of an ADCP to compute suspended-sediment discharge in the tidal Hudson River, New York. *U.S. Geological Survey Scientific Investigations Report 2006-5055: 16*.
- Wood, M.S., Fosness, R.L., Etheridge, A.B. (2015) Sediment transport and evaluation of sediment surrogate ratings in the Kootenai River near Bonners Ferry, Idaho, Water Years 2011–14. *Scientific Investigations Report: 56*. 10.3133/sir20155169
- Wood, M.S., Teasdale, G.N. (2013a) Use of surrogate technologies to estimate suspended sediment in the Clearwater River, Idaho, and Snake River, Washington, 2008-10. *Scientific Investigations Report: 40*. 10.3133/sir20135052
- Wood, M.S., Teasdale, G.N. (2013b) Use of surrogate technologies to estimate suspended sediment in the Clearwater River, Idaho, and Snake River, Washington, 2008–10. *U.S. Geological Survey Scientific Investigations Report 2013-5052: 30*.
- Wright, S.A., Topping, D.J., Williams, C.A. (2010) Discriminating silt-and-clay from suspended-sand in rivers using side-looking acoustic profilers. *Proceedings of the Second Joint Federal Interagency Conference, Las Vegas, Nev. US*.

1	Date	Time	SSC	SSClog	CRLE
2	9/26/2017	3:03	5	0.698970004	CRLE
3	9/26/2017	5:03	23	1.361727836	CRLE
4	9/26/2017	7:03	31	1.491361694	CRLE
5	9/26/2017	9:03	40	1.602059991	CRLE
6	9/26/2017	11:03	50	1.698970004	CRLE
7	9/26/2017	13:03	49	1.69019608	CRLE
8	9/26/2017	15:03	43	1.633468456	CRLE
9	9/26/2017	17:03	34	1.531478917	CRLE
10	9/26/2017	19:03	34	1.531478917	CRLE
11	9/26/2017	21:03	23	1.361727836	CRLE
12	9/26/2017	23:03	21	1.322219295	CRLE
13	9/27/2017	1:03	20	1.301029996	CRLE
14	9/27/2017	3:03	18	1.255272505	CRLE
15	9/27/2017	5:03	21	1.322219295	CRLE
16	9/27/2017	7:03	8	0.903089987	CRLE

Figure A-2: An example of sediment (constituent) data from Oreti River at Taramoa used in SAID tool.

Backscatter profile of the Acoustic Doppler Velocity Meter samples for monitoring sites

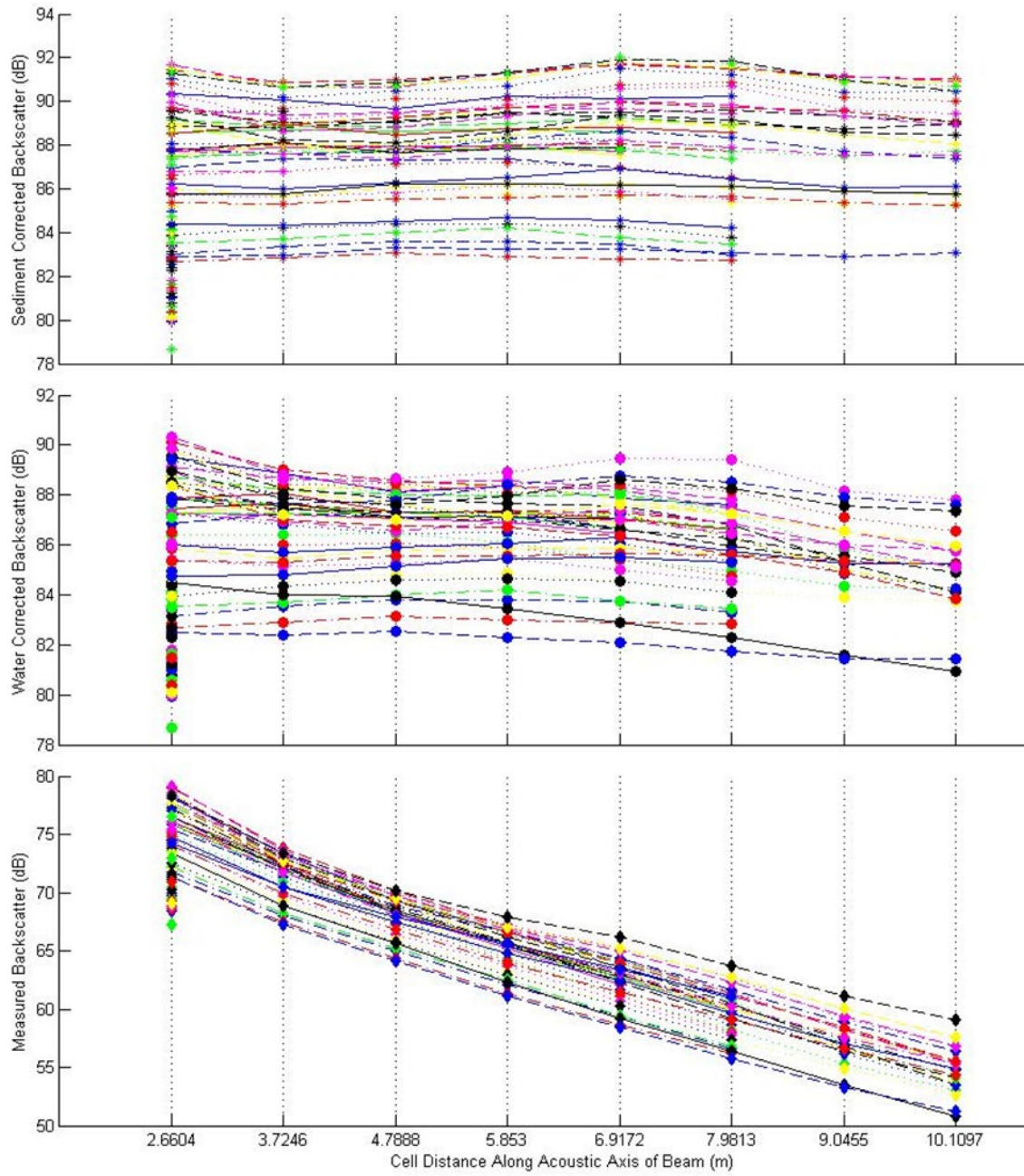


Figure A-3: Backscatter profile of the Acoustic Doppler Velocity Meter samples of the 1200 kHz . side-looking ChannelMaster for the times matching sediment sampling in the Mataura River.

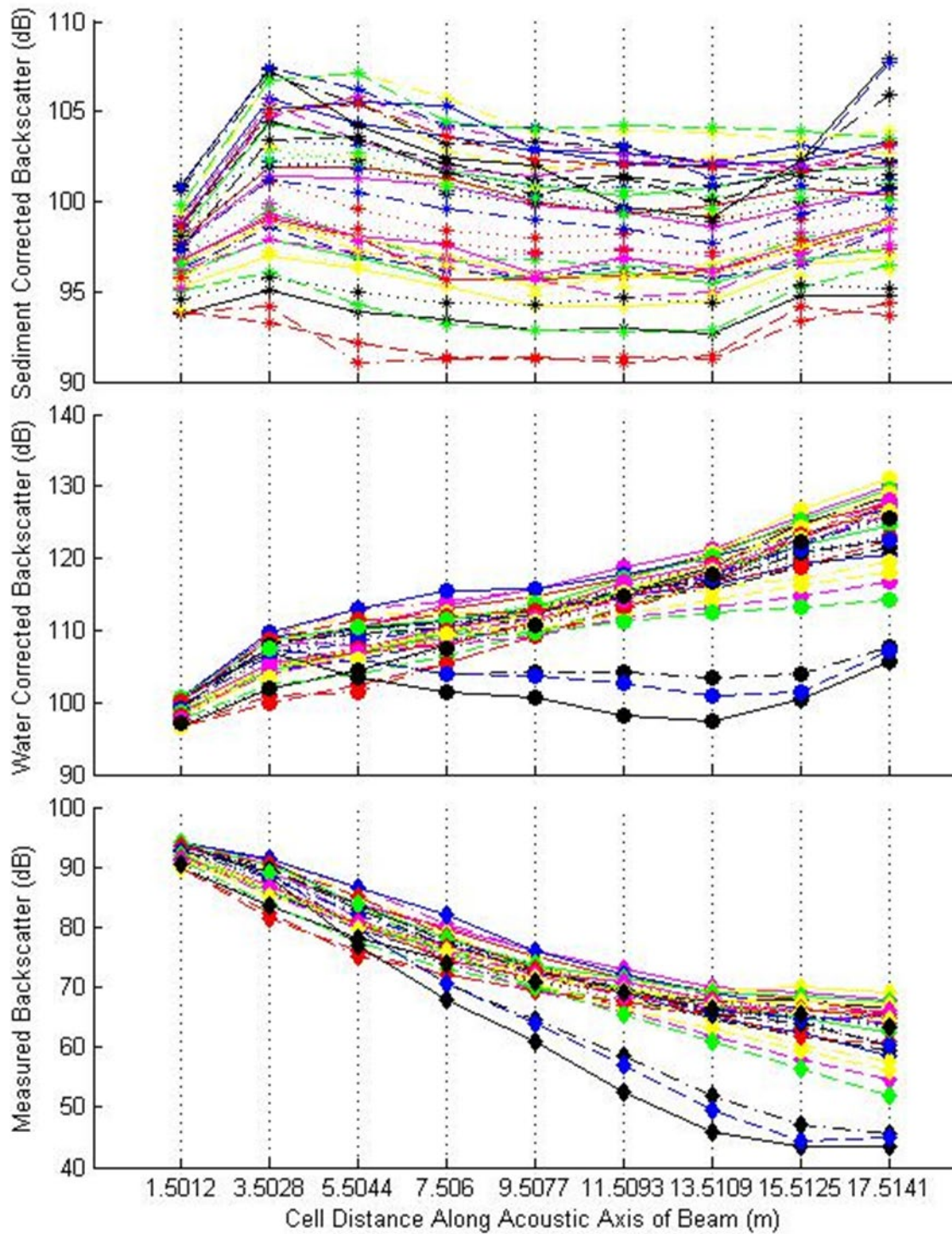


Figure A-4: Backscatter profile of the Acoustic Doppler Velocity Meter samples of the 1500 kHz . side-looking OTT-SLD for the times matching sediment sampling in the Manawatu River.

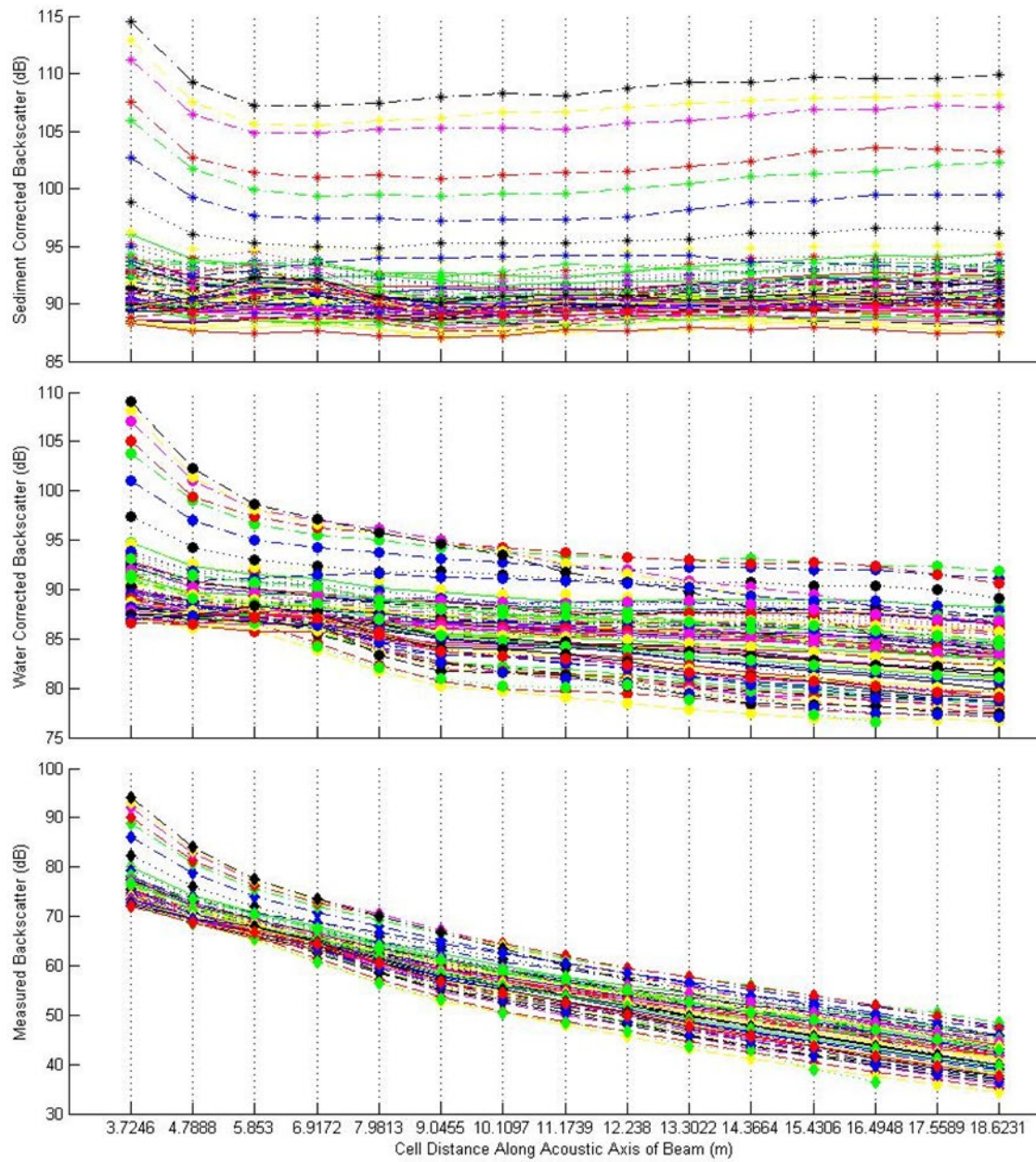


Figure A-5: Backscatter profile of the Acoustic Doppler Velocity Meter samples of the 1200 kHz . side-looking ChannelMaster for the times matching sediment sampling in the Grey River.